LUND UNIVERSITY

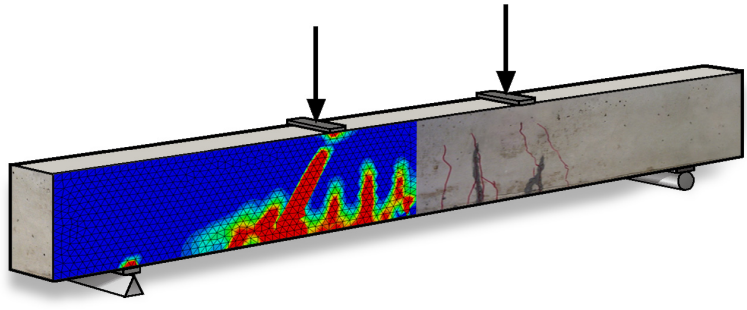

STRUCTURAL RETROFITTING OF REINFORCED CONCRETE BEAMS USING CARBON FIBRE REINFORCED POLYMER

YASMEEN TALEB OBAIDAT

Structural Mechanics

Licentiate Dissertation

Department of Construction Sciences
Structural Mechanics

ISRN LUTVDG/TVSM--10/3070--SE (1-76)
ISSN 0281-6679

STRUCTURAL RETROFITTING OF REINFORCED CONCRETE BEAMS USING CARBON FIBRE REINFORCED POLYMER

YASMEEN TALEB OBAIDAT

Printed by Wallin & Dalholm Digital AB, Lund, Sweden, May, 2010 *(Pl)*.

For information, address:
Division of Structural Mechanics, LTH, Lund University, Box 118, SE-221 00 Lund, Sweden.
Homepage: http://www.byggmek.lth.se

Abstract

This thesis details experimental work and finite element simulations of reinforced concrete beams retrofitted with carbon fibre reinforced polymer (CFRP). The objectives of this study were to investigate the behaviour of retrofitted beams experimentally, develop a finite element model describing the beams, verifying the finite element model against the experimental results and finally investigating the influence of different parameters on the behaviour of the retrofitted beams.

The experimental tests were performed to investigate the behaviour of beams designed in such a way that either flexural or shear failure will be expected. The beams were loaded in four-point bending until cracks developed. The beams were then unloaded and retrofitted with CFRP. Finally the beams were loaded until failure. The ABAQUS program was used to develop finite element models for simulation of the behaviour of beams. The concrete was modelled using a plastic damage model and two models, a perfect bond model and a cohesive model, were evaluated for the concrete-CFRP interface. From the analyses the load-deflection relationships until failure, failure modes and crack patterns were obtained and compared to the experimental results. The FEM results agreed well with the experiments when using the cohesive model regarding failure mode and load capacity while the perfect bond model was not able to represent the debonding failure mode. The results showed that when the length of CFRP increases the load capacity of the beam increases both for shear and flexural retrofitting. FEM results also showed that the width and stiffness of CFRP affect the failure mode of retrofitted beams. The maximum load increases with increased width. Increased CFRP stiffness increases the maximum load only up to a certain value of the stiffness, and thereafter it decreases the maximum load.

Acknowledgements

The financial support provided by the Erasmus Mundus External Cooperation Window Lot 3 is greatly acknowledged.

My most grateful appreciation goes to Professor Ola Dahlblom for his knowledgeable insight and motivating words.

I also feel so lucky and blessed to have Dr. Susanne Heyden as my co-advisor. To me, she is a role model for living and working.

A special thanks to Dr. Kent Persson for his assistance in using the finite element software (ABAQUS). I would also like to thank everyone from Structural Mechanics.

Finally, I would especially like to thank my parents, brothers, sisters and close friends for their love, vote of confidence and support throughout this time. I would also like to share this moment of happiness with my father and mother.

Yasmeen Taleb Obaidat
Lund in May 2010

Contents

1 Introduction

1.1 Background

Reinforced concrete structures often have to face modification and improvement of their performance during their service life. The main contributing factors are change in their use, new design standards, deterioration due to corrosion in the steel caused by exposure to an aggressive environment and accident events such as earthquakes.

In such circumstances there are two possible solutions: replacement or retrofitting. Full structure replacement might have determinate disadvantages such as high costs for material and labour, a stronger environmental impact and inconvenience due to interruption of the function of the structure e.g. traffic problems. When possible, it is often better to repair or upgrade the structure by retrofitting.

In the last decade, the development of strong epoxy glue has led to a technique which has great potential in the field of upgrading structures. Basically the technique involves gluing steel plates or fibre reinforced polymer (FRP) plates to the surface of the concrete. The plates then act compositely with the concrete and help to carry the loads.

FRP can be convenient compared to steel for a number of reasons. These materials have higher ultimate strength and lower density than steel. The installation is easier and temporary support until the adhesive gains its strength is not required due to the low weight. They can be formed on site into complicated shapes and can also be easily cut to length on site.

This work is a study of the behaviour of concrete beams retrofitted with carbon FRP (CFRP), using experiments and finite element modelling.

1.2 Aim and Scope

The overall aim of the present study is to investigate and improve the understanding of the behaviour of reinforced concrete beams retrofitted with CFRP. Experimental tests were performed to investigate the behaviour of beams designed in such a way that either flexural or shear failure will be expected. The beams were loaded in four-point bending until cracks developed. The beams were then unloaded and retrofitted with CFRP. Finally the beams were loaded until failure. The ABAQUS program was used to develop finite element models for simulation of the behaviour of beams. From the analyses the load-deflection relationships until failure, failure modes and crack patterns were obtained and compared to the experimental results. The models were then used to study how different parameters affect retrofitted beam behaviour and investigate how CFRP should be applied in order to get maximum increase of load capacity.

2 Retrofitting of Reinforced Concrete Beams

2.1 FRP Material

Fibre reinforced polymer (FRP) composites consist of high strength fibres embedded in a matrix of polymer resin as shown in Figure 1.

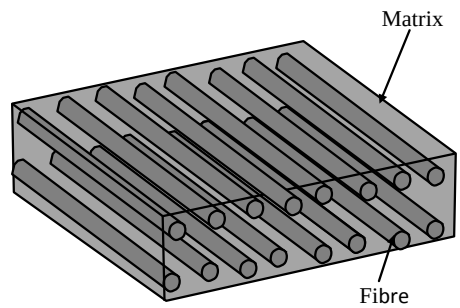

Figure 1: A schematic diagram showing a typical unidirectional FRP plate.

Fibres typically used in FRP are glass, carbon and aramid. Typical values for properties of the fibres are given in Table 1. These fibres are all linear elastic up to failure, with no significant yielding compared to steel. The primary functions of the matrix in a composite are to transfer stress between the fibres, to provide a barrier against the environment and to protect the surface of the fibres from mechanical abrasion. Typical properties for epoxy are given in Table 1.

The mechanical properties of composites are dependent on the fibre properties, matrix properties, fibre-matrix bond properties, fibre amount and fibre orientation. A composite with all fibres in one direction is designated as unidirectional. If the fibres are woven, or oriented in many directions, the composite is bi- or multidirectional. Since it is mainly the fibres that provide stiffness and strength composites are often anisotropic with high stiffness in the fibre direction(s). In strengthening applications, unidirectional composites are predominantly used, Figure 1. The approximate stiffness and strength of a unidirectional CFRP with a 65% volume fraction of carbon fibre is given in Table 1. As a comparison the corresponding properties for steel are also given.

Adhesives are used to attach the composites to other surfaces such as concrete. The most common adhesives are acrylics, epoxies and urethanes. Epoxies provide high bond strength with high temperature resistance, whereas acrylics provide moderate temperature resistance with good strength and rapid curing. Several considerations are involved in applying adhesives effectively. Careful surface preparation such as removing the cement paste, grinding the surface by using a disc sander, removing the dust generated by surface grinding using an air blower and carful curing are critical to bond performance.

Table 1. Typical strength and stiffness values for materials used in retrofitting, [1].

Material	Tensile strength (MPa)	Modulus of elasticity (GPa)	Density (kg/m^3)	Modulus of elasticity to density ratio (Mm^2/s^2)
Carbon	2200-5600	240-830	1800-2200	130-380
Aramid	2400-3600	130-160	1400-1500	90-110
Glass	3400-4800	70-90	2200-2500	31-33
Epoxy	60	2.5	1100-1400	1.8-2.3
CFRP	1500-3700	160-540	1400-1700	110-320
Steel	280-1900	190-210	7900	24-27

2.2 Application in Retrofitting

For structural applications, FRP is mainly used in two areas. The first area involves the use of FRP bars instead of steel reinforcing bars or pre-stressing strands in concrete structures. The other application, which is the focus of this thesis, is to strengthen structurally deficient structural members with external application of FRP.

Retrofitting with adhesive bonded FRP has been established around the world as an effective method applicable to many types of concrete structural elements such as columns, beams, slabs and walls. As an example, a highway RC bridge slab in China was retrofitted using CFRP as shown in Figure 2(a) and a column in India was retrofitted using glass FRP wrapping as shown in Figure 2(b), [2].

FRP plates can be bonded to reinforced concrete structural elements using various techniques such as external bonding, wrapping and near surface mounting. Retrofitting with externally bonded FRP has been shown to be applicable to many types of RC structural elements. FRP plates or sheets may be glued to the tension side of a structural member to provide flexural strength or glued to the web side of a beam to provide shear strength. FRP sheets can also be wrapped around a beam to provide shear strength and be wrapped around a column to provide confinement and thus increase the strength and ductility. Near surface mounting consists of sawing a longitudinal groove in a concrete member, applying a bonding material in the groove and inserting an FRP bar or strip.

(a) Flexural strengthening of a highway RC bridge slab in China.

(b) Seismic retrofit of supporting columns for a cryogenic tank in Gujarat, India.

Figure 2. Examples of use of FRP in existing structures, [2].

3 Related Research

3.1 Experimental Work

Investigation of the behaviour of FRP retrofitted reinforced concrete structures has in the last decade become a very important research field. In terms of experimental application several studies were performed to study the behaviour of retrofitted beams and how various parameters influence the behaviour.

The effect of number of layers of CFRP on the behaviour of a strengthened RC beam was investigated by Toutanji et al. [3]. They tested simply supported beams with different numbers of CFRP layers. The specimens were subjected to a four-point bending test. The results showed that the load carrying capacity increases with an increased number of layers of carbon fibre sheets.

Investigation of the effect of internal reinforcement ratio on the behaviour of strengthened beams has been performed by Esfahani et al. [4]. Specimens with different internal steel ratio were strengthened in flexure by CFRP sheets. The authors reported that the flexural strength and stiffness of the strengthened beams increased compared to the control specimens. With a large reinforcing ratio, they also found that failure of the strengthened beams occurred in either interfacial debonding induced by a flexural shear crack or interfacial debonding induced by a flexural crack.

A test programme on retrofitted beams with shear deficiencies was done by Khalifa et al. [5]. The experimental results indicated that the contribution of externally bonded CFRP to the shear capacity of continuous RC beams is significant.

There are three main categories of failure in concrete structures retrofitted with FRP that have been observed experimentally, Esfahani et al. [4], Ashour et al. [6], Garden and Hollaway, [7], Smith and Teng, [8]. The first and second type consist of failure modes where the composite action between concrete and FRP is maintained. Typically, in the first failure mode, the steel reinforcement yields, followed by rupture of CFRP as shown in Figure 3(a). In the second type there is failure in the concrete. This type occurs either due to crushing of concrete before or after yielding of tensile steel without any damage to the FRP laminate, Figure 3(b), or due to an inclined shear crack at the end of the plate, Figure 3(c). In the third type, the failure modes involving loss of composite action are included. The most recognized failure modes within this group are debonding modes. In such a case, the external reinforcement plates no longer contribute to the beam strength, leading to a brittle failure if no stress redistribution from the laminate to the interior steel reinforcement occurs. Figures 3(d)-(g) show failure modes of the third type for RC beams retrofitted with FRP. In Figure 3(d), the failure starts at the end of the plate due to the stress concentration and ends up with debonding propagation inwards. Stresses at this location are essentially shear stress but due to small but non-zero bending stiffness of the laminate, normal stress can arise. For the case in

Figure 3(e) the entire concrete cover is separated. This failure mode usually results from the formation of a crack at or near the end of the plate, due to the interfacial shear and normal stress concentrations. Once a crack occurs in the concrete near the plate end, the crack will propagate to the level of tensile reinforcement and extend horizontally along the bottom of the tension steel reinforcement. With increasing external load, the horizontal crack may propagate to cause the concrete cover to separate with the FRP plate. In Figures 3(f) and (g) the failure is caused by crack propagation in the concrete parallel to the bonded plate and adjacent to the adhesive to concrete interface, starting from the critically stressed portions towards one of the ends of the plate. It is believed to be the result of high interfacial shear and normal stresses concentrated at a crack along the beam. Also mid span debonding may take concrete cover with it.

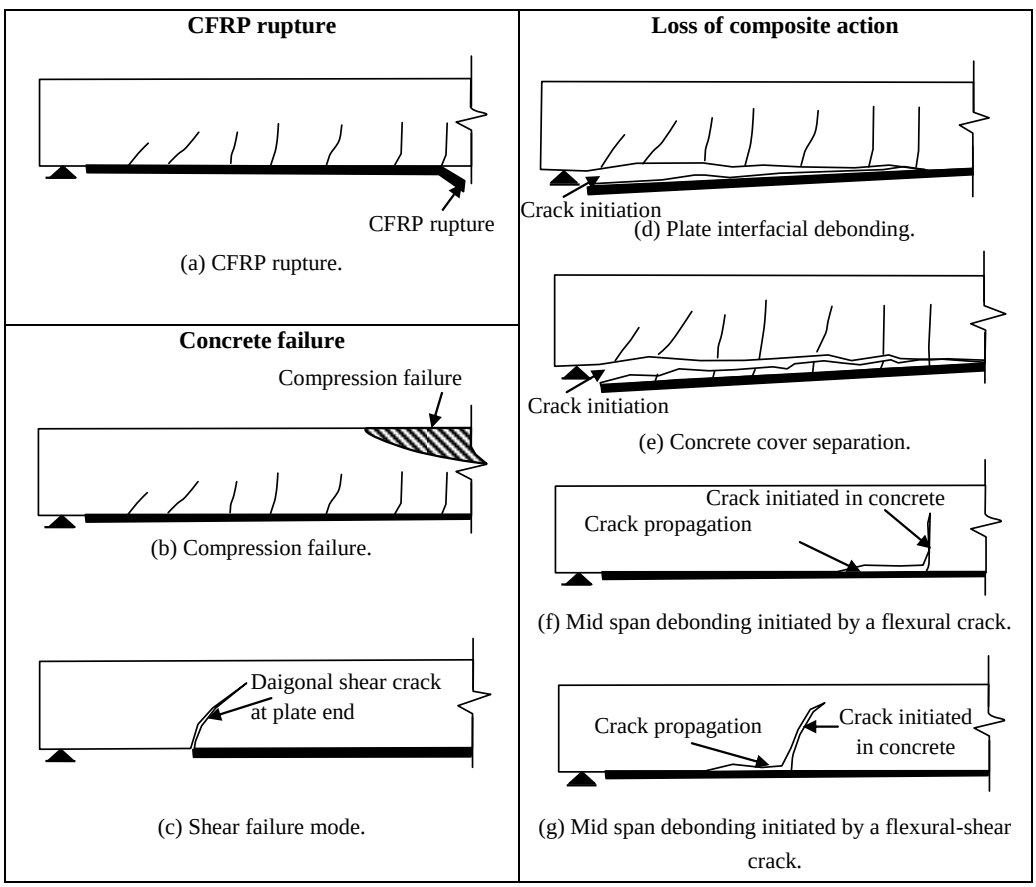

Figure 3: Failure modes in beam retrofitted in flexure.

3.2 Modelling Work

Many models currently exist for reinforced concrete retrofitted with CFRP. Several different approaches have been considered. Some models use simple material models and are restricted to 2D and others use nonlinear elasticity or plasticity models to capture the more complicated effects and predict the behaviour of retrofitted reinforced concrete in a general sense. Each approach has its strengths, complexity level, and complications.

A 2D model was developed by Supaviriyakit et al. [9] for analyses of RC beams strengthened with externally bonded FRP plates. The RC element considered the effect of crack and reinforcing steel as being smeared over the entire element. Perfect compatibility between cracked concrete and reinforcing steel was assumed. The FRP plate was modelled as an elastic brittle element. As the epoxy is usually stronger than the concrete, perfect bond between FRP and concrete was assumed.

The orthotropic properties of FRP were taken into consideration by Hu et al. [10] in modelling the behaviour of a retrofitted beam. They assumed perfect bond between the CFRP plate and concrete.

The effect of anchorage length of near surface mounted reinforcement (NSMR) was studied by Lundqvist et al. [11]. They conducted numerical analyses of three different CFRP strengthening techniques to find a critical anchorage length, where a longer anchorage length does not contribute to the load bearing capacity. They assumed perfect bond between the plate and concrete. The results showed that a critical anchorage length exists for plates and sheets as well as for NSMR.

Bond is a critical parameter in strengthening systems as it provides the shear transfer between concrete and FRP necessary for composite action. Lim et al. [12] presented a numerical model to simulate the interface fracture behaviour of concrete strengthened with external composite plates. They adapted the fictitious crack model, [13] with a nonlinear fracture mechanics concept to describe the constitutive relationship at the element level. They found that the interface material properties had significant influence on the interface stress distributions. Furthermore, Camata et al. [14], investigated RC members strengthened in flexure by FRP plates. The model considers the actual crack patterns observed in the test using a smeared and interface crack model. The results show that debonding and concrete cover splitting failure mode always occur by crack propagation inside the concrete. A FE analysis was performed by Neale et al. [15], to simulate the nonlinear behaviour of shear strengthened beams and two-way slabs. A plasticity–based concrete constitutive model was used. An elastic–plastic response was assumed for the steel and the CFRP was modelled as linear elastic until failure. A bond slip model was incorporated to the analysis to simulate the FRP concrete interface.

3.3 Discussion

Even though extensive work has been done on the use of CFRP laminates in retrofitting there is a need for further refinement of models and further parameter studies. From the above literature review, it can be concluded that the interface zone has been modelled with linear or in 2D with non-linear models. The present study comprises a 3D cohesive model which is believed to better reflect the behaviour of retrofitted beams.

In practical use of retrofitting, the structure is often damaged at the time of retrofitting. To take account of this, the beams in the experimental study as well as in the simulations were pre-cracked before retrofitting. This has not been done before in connection with retrofitting in shear or investigation of influence of CFRP length.

Researchers have reported on different failure modes. It is important to understand under what circumstances a certain failure mode will occur. To contribute to this understanding, a parametric study of the influence of CFRP stiffness and width is included in this simulation work.

4 Summary of the Papers

Paper A Obaidat, Y.T., Heyden, S., Dahlblom, O., Abu-Farsakh, G., and Abdel-Jawad, Y.: Retrofitting of reinforced concrete beams using composite laminates. Submitted to *Construction & Building Materials*, 2010.

Summary: This paper presents the results of an experimental study to investigate the behaviour of structurally damaged full-scale reinforced concrete beams retrofitted with CFRP laminates in shear or in flexure. The main variables considered were the internal reinforcement ratio, position of retrofitting and the length of CFRP. The experimental results, generally, indicate that beams retrofitted in shear and flexure by using CFRP laminates are structurally efficient and are restored to stiffness and strength values nearly equal to or greater than those of the control beams. It was found that the efficiency of the strengthening technique by CFRP in flexure varied depending on the length. The main failure mode in the experimental work was plate debonding in retrofitted beams.

Paper B Obaidat,Y.T., Heyden, S. and Dahlblom, O.: The Effect of CFRP and CFRP/ Concrete Interface Models when Modelling Retrofitted RC Beams with FEM. Published in *Composite Structures*, 2010; 92: 1391–1398.

Summary: This paper presents a finite element analysis which is validated against laboratory tests of eight beams. All beams had the same rectangular cross-section geometry and were loaded under four point bending, but differed in the length of the carbon fibre reinforced plastic (CFRP) plate. The commercial numerical analysis tool Abaqus was used, and different material models were evaluated with respect to their ability to describe the behaviour of the beams. Linear elastic isotropic and orthotropic models were used for the CFRP and a perfect bond model and a cohesive bond model was used for the concrete–CFRP interface. A plastic damage model was used for the concrete. The analyses results show good agreement with the experimental data regarding load–displacement response, crack pattern and debonding failure mode when the cohesive bond model is used. The perfect bond model failed to capture the softening behaviour of the beams. There is no significant difference between the elastic isotropic and orthotropic models for the CFRP.

Paper C Obaidat,Y.T., Dahlblom, O. and Heyden, S.: Nonlinear FE modelling of shear behaviour in RC beam retrofitted with CFRP. Computational Modelling of Concrete Structures conference (EURO-C 2010), 2010.

Summary: To examine numerically the behaviour of beams retrofitted in shear and the effects of length and orientation of CFRP in the beams, in this paper a nonlinear 3-D numerical model has been developed using the ABAQUS finite element program. Two models were used to represent the interface between CFRP and concrete, a perfect bond model and a cohesive model. Validation of the model was performed using data obtained from an experimental study. The results showed that the cohesive model is able to simulate the composite behaviour of reinforced concrete beams retrofitted by CFRP in shear correctly. The model is then used to examine the influence of length and orientation of CFRP. It is shown that the length of CFRP and the orientation strongly influence on the behaviour of the retrofitted beams.

Paper D Obaidat,Y.T., Heyden, S. and Dahlblom, O.: FEM Study on the Effect of CFRP Stiffness and Width on Retrofitted Reinforced Concrete Beam Behaviour. Submitted to *Composite Structures,* 2010.

Summary: The finite element program ABAQUS was used to study the effect of different parameters on the behaviour of an RC beam retrofitted with carbon fibre reinforced polymer (CFRP). These parameters were the stiffness and width of the CFRP. A linear elastic isotropic model was used for the CFRP and a cohesive bond model was used for the concrete–CFRP interface. A plastic damage model was used for the concrete. The material models were validated against experimental work and the results showed good agreement between experimental data and numerical results. Observations indicate that the CFRP width to beam width ratio and CFRP stiffness influence the type of failure mode of a beam retrofitted with CFRP. For small width and for large value of stiffness debonding will occur before steel yielding due to stress concentration at the end of the plate. For small values of stiffness rupture of CFRP will occur. It was found that when the stiffness of CFRP increases the maximum load increases until a certain value of stiffness, then the maximum load decreases again. Simulations also show that the external load at steel yielding and the maximum load increase with the CFRP width.

5 Conclusions and Future Work

5.1 Conclusions

The finite element method is a useful tool for improving the understanding of the behaviour of reinforced concrete beams retrofitted with CFRP. Experimental tests are needed to provide input data to the model and for the purpose of verification of simulation results. When the model has been validated it can be used for parameter studies to clarify the influence of various parameters.

The plastic damage model used for concrete and the elastic-perfectly plastic model used for steel proved to be able to model the reinforced concrete, as was shown by comparing simulations to tests of control beams. A uni-axial CFRP is essentially an orthotropic material, but simulations showed that for cases where the principal stress direction coincides with the fibre direction, an isotropic model could be used with good accuracy.

Since debonding plays an important role as a limiting phenomenon for retrofitted beams, a perfect bond model is not suitable for the CFRP-concrete interface, at least not if the intention is to study the fracture behaviour. The cohesive bond model, on the other hand, can capture the debonding and simulations using this model showed good agreement with experiments concerning stiffness, maximum load, crack patterns and failure mode.

Experiments and simulations showed that retrofitting can increase load capacity and stiffness and the effect is larger for retrofitting in flexure than in shear. On the other hand, simulations showed that an increase in the amount of CFRP will in some cases decrease the maximum load. This means that understanding of the behaviour of a retrofitted structure is very important since an unsuitable arrangement of CFRP can actually make the situation worse.

Experiments and simulations showed that it is important to provide a sufficient anchorage length outside the region of maximum stress to obtain full effect from the retrofitting. For retrofitting in shear, it was also shown that the best effect is obtained it the fibre direction of the CFRP coincides with the principal tensile stress direction.

Simulations showed that several different failure modes can occur, depending on the geometry and stiffness properties of the CFRP. Many of the failure modes involve debonding, associated with a stress concentration in the concrete-CFRP interface zone. An important criterion when designing the CFRP arrangement is thus to avoid stress concentrations as far as is possible. A high stiffness and low width of the CFRP will give a pronounced stress concentration at the plate end. This should definitely be avoided since it will cause debonding before steel yielding and failure will occur at low load.

A wider CFRP plate will (for constant stiffness) always give a higher maximum load, while increased CFRP stiffness will increase the maximum load only up to a certain value of the stiffness, and thereafter it will decrease the maximum load.

5.2 Future Work

Since debonding is such an important phenomenon when retrofitting with CFRP is concerned, more attention should be given to the behaviour of the concrete-CFRP bond. More experimental data on the micro-level is needed to provide the information needed for further developing the material model used for the interface. Another interesting area when it comes to developing the model is usage of the extended finite element method (XFEM) to represent the cracks in the concrete.

A parametric study in this work took into consideration the effect of varying the stiffness properties and geometry of the CFRP on the type of failure and stress concentrations. It would also be interesting to study the effect of beam stiffness properties and geometry on the behaviour of a beam, stress concentrations and type of failure.

This study showed that there is a stress concentration at the end of the plate causing debonding failure. It would be interesting to study different approaches to avoid this phenomenon. Examples are tapering at end of plate and external CFRP wrapping (stirrup) for reducing the stress concentration at the end of the plate.

Previous experimental programmes have shown that the CFRP plate retrofitting system enhances the capacity of deficient concrete beams. There are, however, many environmental factors involved during the life span of a retrofitted structure that needs more attention. They include seasonal temperature variation, degradation of material properties, creep and so on. The durability of CFRP reinforced beams under these conditions should be investigated.

References

[1] Piggott, M.: Load bearing fibre composites, 2nd Edition. Kluwer Academic Publishers, Boston/ Dordrecht/ London. 2002.

[2] Karbhari, M.: FRP International. The Official Newsletter of the International Institute for FRP in Construction. 2004; 1(2).

[3] Toutanji, H., Zhao, L., and Zhang, Y.: Flexural behavior of reinforced concrete beams externally strengthened with CFRP sheets bonded with an inorganic matrix. *Engineering Structures*. 2006; 28: 557-566.

[4] Esfahani, M., Kianoush, M., and Tajari, A.: Flexural behaviour of reinforced concrete beams strengthened by CFRP sheets. *Engineering structures.* 2007, 29: 2428-2444.

[5] Khalifa, A., Tumialan, G., Nanni, A. and Belarbi, A.: Shear Strengthening of Continuous RC Beams using Externally Bonded CFRP Sheet. *American Concrete Institute, Proc., 4th International Symposium on FRP for Reinforcement of Concrete Structures (FRPRCS4), Baltimore, MD*, Nov. 1999: 995-1008.

[6] Ashour AF, El-Refaie S.A., and Garrity, S.W.: Flexural strengthening of RC continuous beams using CFRP laminates. *Cement & Concrete Composites.* 2004; 26:765-775.

[7] Garden, H.N., and Hollaway, L.C.: An Experimental Study of the Influence of Plate End Anchorage of Carbon Fiber Composite Plates used to Strengthen Reinforced Concrete Beams. Composite Structures. 1998, 42, 2, 175-88.

[8] Smith, S.T., and Teng, J.G.: FRP-Strengthened RC Beams I: Review of Debonding Strength Models. Engineering Structures. 2002, 24, 4, 385-95.

[9] Supaviriyakit, T., Pornpongsaroj, P., and Pimanamas, A.: Finite Element Analysis of FRP Strengthened RC Beam. *Songklanakarin J.Sci.Technol.* 2004, 26(4): 497-507.

[10] Hu, H.-T., Lin, F.-M., & Jan, Y.-Y.: Nonlinear finite element analysis of reinforced concrete beams strengthened by fiber–reinforced plastics. *Cement and concrete composite.* 2006, 28: 102-114.

[11] Lundquist, J., Nordin, H., Täljsten, B., and Olofsson, T.: Numerical analyis of concrete beams sterengthened with CFRP- A Study of anchorage lengths. *In: FRP in Construction, Proceeding of The International Symposium of Bond Behaviour of FRP in Structures*. 2005; 247-254.

[12] Lim, Y., Shin, S., and Kim, M.: A study on the effect of externally bonded composite plate-concrete interface. *Composite Structures.* 2008, 82:403-412.

[13] Hillerborg, A., Modéer, M., and Petersson, P.E.: Analysis of crack formation and crack growth in concrete by means of fracture mechanics and finite elements. *Cement Concrete.* 1976, 6: 773–782.

[14] Camata, G., Spacone, E., and Zarnic, R.: Experimental and nonlinear finite element studies of RC beams strengthened with FRP plates. *Composites: Part B.* 2007, 38: 277-288.

[15] Neale, K., Ebead, U., Abdel Baky, H., Elsayed, W., and Godat, A.: Modelling of debonding phenomena in FRP-strengthened concrete beams and slabs. *Proceeding of the international symposium on bond behaviour of FRP in structures (BBFS)*. 2005.

Paper A

A

Retrofitting Of Reinforced Concrete Beams Using Composite Laminates

Yasmeen Taleb Obaidat, Susanne Heyden, Ola Dahlblom, Ghazi Abu-Farsakh and Yahia Abdel-Jawad

Submitted to Construction & Building Materials

Retrofitting of Reinforced Concrete Beams using Composite Laminates

Yasmeen Taleb Obaidat[a,*], Susanne Heyden[a], Ola Dahlblom[a], Ghazi Abu- Farsakh[b] and Yahia Abdel-Jawad[b]

[a] Division of Structural Mechanics, Lund University, Lund, Sweden

[b] Jordan University of Science and Technology, Irbid, Jordan

Abstract:

This paper presents the results of an experimental study to investigate the behaviour of structurally damaged full-scale reinforced concrete beams retrofitted with CFRP laminates in shear or in flexure. The main variables considered were the internal reinforcement ratio, position of retrofitting and the length of CFRP. The experimental results, generally, indicate that beams retrofitted in shear and flexure by using CFRP laminates are structurally efficient and are restored to stiffness and strength values nearly equal to or greater than those of the control beams. It was found that the efficiency of the strengthening technique by CFRP in flexure varied depending on the length. The main failure mode in the experimental work was plate debonding in retrofitted beams.

Keywords: Carbon Fibre Reinforced Plastic (CFRP), Strengthening, Retrofitting, Laminate, Reinforced Concrete Beam, Flexure, Debonding.

1. Introduction:

There are many existing structures, which do not fulfill specified requirements. This may for example be due to upgrading of the design standards, increased loading, corrosion of the reinforcement bars, construction errors or accidents such as earthquakes. To remedy for insufficient capacity the structures need to be replaced or retrofitted.

Different types of strengthening materials are available in the market. Examples of these are ferrocement, steel plates and fibre reinforced polymer (FRP) laminate. Retrofitting of reinforced concrete (RC) structures by bonding external steel and FRP plates or sheets is an effective method for improving structural performance under both service and ultimate load conditions. It is both environmentally and economically preferable to repair or strengthen structures rather than to replace them totally. With the

* Corresponding author.
E-mail address: Yasmeen.Obaidat@construction.lth.se

development of structurally effective adhesives, there have been marked increases in strengthening using steel plates and FRP laminates. FRP has become increasingly attractive compared to steel plates due to its advantageous low weight, high stiffness and strength to weight ratio, corrosion resistance, lower maintenance costs and faster installation time.

Earlier research has demonstrated that the addition of carbon fibre reinforced polymer (CFRP) laminate to reinforced concrete beams can increase stiffness and maximum load of the beams. In a study by Toutanj et al. [1] beams retrofitted with CFRP laminates showed an increased maximum load up to 170 % as compared to control beams. Another study by Kachlakev and McCurry [2] shows an increase of 150 % when beams were strengthened in both flexure and shear with CFRP and glass FRP laminates respectively. Other studies have also been conducted by David et al. [3], Shahawy et al. [4], Khalifa and Nanni [5], Shehata et al. [6], Khalifa et al. [7] in an attempt to quantify the flexural and shear strengthening enhancements offered by the externally bonded CFRP laminates. Ferreira et al. [8] showed that when a beam is strengthened with CFRP sheets the stiffness increase and the tension cracking is delayed to higher loads, and Karunasena et al. [9] showed that an externally bonded composite, of either CFRP or GFRP materials, improved the moment capacity of deteriorated concrete beams.

In spite of many studies of the behaviour of retrofitted beams, the effect of the length of CFRP on the behaviour of pre-cracked beams retrofitted by CFRP in flexure and the behaviour of retrofitted beams in shear after preloading have not been explored. This study examined experimentally the flexural and the shear behaviours of RC-beams retrofitted or strengthened with CFRP laminates. To accomplish this, laboratory testing was conducted on full-size beams. The main variables in this study are the reinforcement steel ratio and CFRP length.

2. Material and methods

The experimental work undertaken in this study consisted of four point bending tests of twelve simply supported RC beams. In addition, material tests were carried out to determine the mechanical properties of the concrete, reinforcement steel and CFRP which were used in constructing the beams.

2.1 Materials

An ordinary strength concrete mix was prepared using Ordinary Portland cement (Type I). The aggregate used consisted of coarse limestone, crushed limestone and silica sand. The gradation of coarse and fine particles met the ASTM specification (C136) [10].

The concrete mix was designed according to ACI method 211 [11], to have slump 50 mm and 28 days cylinder compressive strength of 30 MPa. The maximum aggregate size was 10 mm and the free water cement ratio was 0.55. The concrete mix is shown in Table 1.

Table 1 Concrete mix proportions, kg per m^3 concrete.

Materials	**kg/m^3**
Cement	332
Water	206
Coarse Aggregate(5 mm ≤ d ≤ 10 mm)	830
Fine Aggregate (d < 5mm)	662

The mean compressive strength was determined in compressive tests 28 days after casting of three 300 mm by 150 mm diameter cylinders. The average concrete compressive strength was 29 MPa. The failure of a specimen is shown in Fig. 1.

Fig. 1. Concrete specimen in cylinder compression test.

The steel bars used for longitudinal reinforcement were tested in uniaxial tension. Details of the material properties for the reinforcing steel are given in Table 2. The average elastic modulus was 209 GPa. The stirrups were fabricated using steel with nominal diameter 8 mm. This steel was not tested in the experimental work.

Table. 2 **.**Mechanical properties of steel bars.

Nominal Diameter (mm)	**Elastic Modulus (GPa)**	**Yield Stress (MPa)**	**Ultimate Stress (MPa)**	**Ultimate Strain**
10	211	520	741	0.151
12	207	495	760	0.167
18	209	512	739	0.131

The CFRP used in this study was supplied by FOSROC [12]. The laminate had a thickness of 1.2 mm, a width of 50 mm and the elastic modulus 165 GPa according to the manufacturer. The plates were supplied in a roll form as shown in Fig. 2. Three specimens were prepared

and tested using a tension testing machine at a rate of 2 mm/min, to determine the ultimate stress. The mean ultimate stress of the three specimens was 2640 MPa, with the strain corresponding to the failure load being 0.0154. This test also showed that the behaviour of the CFRP is linear elastic up to failure. The failure of a specimen is shown in Fig. 3.

Fig. 2. Roll of CFRP plate.

Fig. 3. The failure of a CFRP laminate specimen.

The material used for the bonding of CFRP plates to the concrete was an epoxy adhesive with compressive strength equal to 40 MPa according to the manufacturer and it was applied with a total thickness equal to 1 mm.

2.2 Experimental Procedure

Twelve beams were tested under four point bending after curing six months. The beams were divided into two groups. For group RF, focus was on flexural behaviour, and for group RS focus was on shear behaviour.

For group RF, two beams were used as control beams. The other six were preloaded until flexural cracks appeared and then retrofitted with CFRP. Three different lengths of CFRP were used, with two nominally equal beams for each length. Finally, the retrofitted beams were loaded until failure and the results were compared with the control beams.

For group RS, two beams were used as control beams, and the other two were preloaded until shear cracks appeared and then retrofitted and finally tested to failure.

2.2.1 Manufacture of beams

The beams had a rectangular cross-section of 150 mm width and 300 mm height, and were 1960 mm long. The beams in group RF were designed to have insufficient flexural strength to obtain a pure flexural failure. They had tension reinforcement (2ϕ12), compression reinforcement (2ϕ10) and the steel bars were tied together with 8 mm stirrups c/c 100 mm along the beam, see Fig. 4(a).

The beams in group RS had the same geometry, but were cast with a reduced shear reinforcement ratio and a larger longitudinal reinforcement ratio in order to obtain pure diagonal shear cracks without development of flexural cracks. The beams had tension reinforcement (2ϕ18), compression reinforcement (2ϕ10) and were tied with 8 mm stirrups c/c 400 mm along the beam as shown in Fig. 4. All beams were designed according to [13].

In all the beams, the clear concrete cover to the main flexural reinforcement was set to 25 mm. This cover was expected to avoid splitting bond failure. Geometry and reinforcement are shown in Fig. 4(b). The beams cured for six months before they were tested.

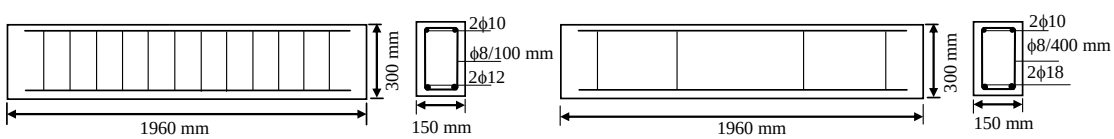

(a) Beams in group RF. (b) Beams in group RS.

Fig. 4. Geometry and reinforcement of beams in groups RF and RS.

2.2.2 Testing of control beams

The beams were tested in four point bending. This load case was chosen because it gives constant maximum moment and zero shear in the section between the loads, and constant maximum shear force between support and load. The moment was linearly varying between supports and load. The span between the supports was 1560 mm and the load was applied at points dividing the length into three equal parts as shown in Fig. 5. Steel plates were used under the loads to distribute the load over the width of the beam. The testing equipment was a

testing machine of 400 kN capacity jack. A linearly variable differential transducer, LVDT, was used to measure the deflection at midspan, as shown in Fig. 5. Fig. 6 shows the test setup of a beam.

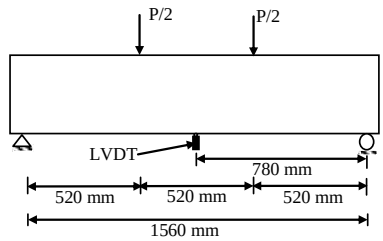

Fig. 5. Supports, loading and position of LVDT.

Fig. 6. Test setup.

Deflections and load were recorded during the test. The first crack appeared in the control beams of group RF at P=60 kN and flexural cracks had formed along the beam at P=95 kN.

For the beams in group RS, shear cracks were initiated in both shear spans. The first shear crack was the critical crack in the beam and it started to develop at P=120 kN. The load in this group is higher than for those in group RF due to intensive flexural reinforcement. A steel ratio around the balanced steel ratio was used.

2.2.3 Preloading of beams

In order to simulate damage, the beams were preloaded before retrofitting. The preloading was done with the same setup as described in 2.2.2. First the beams were loaded until cracks appeared; the load was 95 kN for beams in group RF and for beams in group RS the first shear crack initiated at a load of 120 kN, as determined in the control beams test. Then the load was released.

2.2.4 Retrofitting of beams

The beams in group RF were removed from the test machine and turned over to retrofit them with CFRP as shown in Fig. 7. The soffit of the beam was retrofitted with CFRP laminates 50 mm wide and of three different lengths, 1560 mm (series RF1), 1040 mm (series RF2) and 520 mm (series RF3) as shown in Fig. 7. The laminate was positioned at the centre of the beam width as shown in Fig.8. The laminate was applied when the beams were subjected to a negative moment corresponding to their own dead weight. This implies a small prestressing effect which could be obtained by a jack in the case of on-site repair.

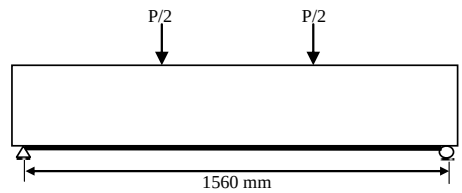

(a) Test series RF1

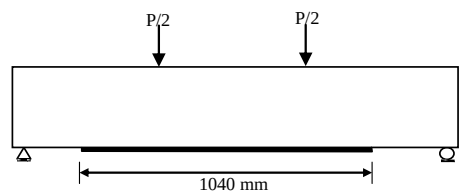

(b) Test series RF2

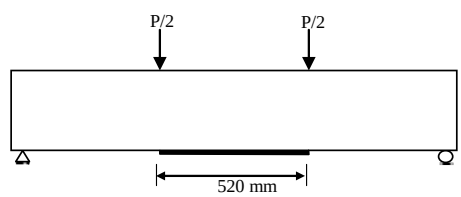

(c) Test series RF3

Fig. 7. Lengths of CFRP laminate in test series RF1, RF2 and RF3.

Fig. 8. Application of CFRP laminate for beams in group RF.

For the beams in group RS, the web of the beam was retrofitted with CFRP laminates 50 mm wide and 300 mm long on the two faces of beams as shown in Fig. 9 and Fig. 10. The same procedure was used as for the beams in group RF, but the position of the laminate was different.

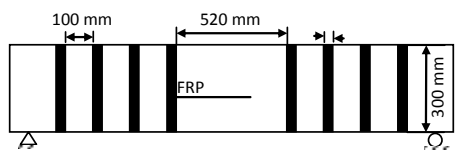

Fig. 9. The arrangement of the CFRP laminate in group RS.

Fig. 10. CFRP laminate in test series RS1.

In order to ensure correct application of the external strengthening materials, it was considered necessary to improve the concrete surface characteristics on the contact areas to be bonded. The surface preparation was done according to the manufacturer's instruction [12]. It included removing the cement paste, grinding the surface by using a disc sander, and removing the dust generated by surface grinding using an air blower. After that the epoxy

adhesive was applied to both the CFRP and the concrete surface. Finally the CFRP plates were applied to the beams.

2.2.5 Testing of retrofitted beams

After 7 days curing at ambient temperature the beams were retested under four point bending until failure occurred. The tests were performed using the same setup as described in section 2.2.2.

3. Results

3.1 Beams in group RF

3.1.1 Control Beams

The load versus midspan deflection curves for the two control beams are shown in Fig. 11. The beams behave in a ductile manner and gives large deflection before the final failure. This is the typical behaviour of an under-reinforced RC member [14]. The difference between the two specimens is rather small, and the mean value, also indicated in the figure, will be used.

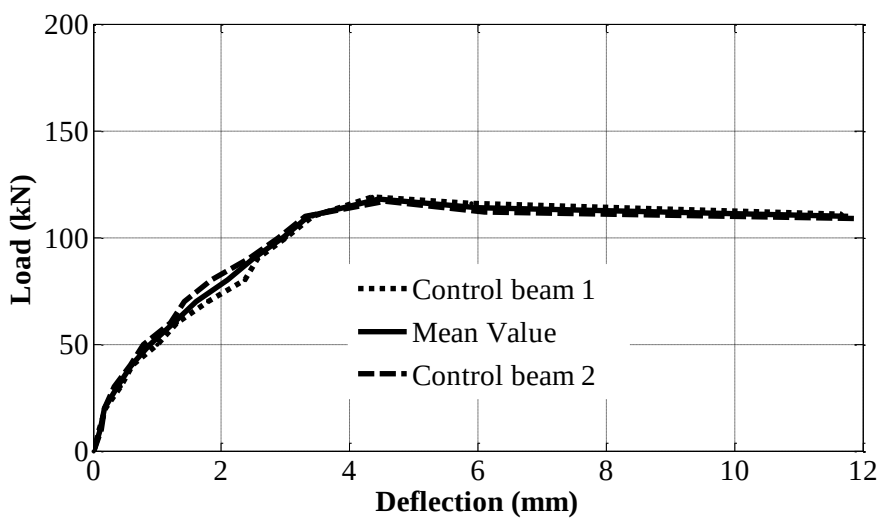

Fig. 11. Comparison between individual control beams in group RF.

The curve includes a linear response up to the load 22 kN. The appearance of a crack was first noted at load 60 kN. The midspan deflection curve illustrates the nonlinearities at

cracking of the concrete. After 95 kN load flexural cracks formed and widened as loading increased. The maximum load was 118 kN as shown in the figure. After maximum load, the cracks did not grow in length for the remainder of the test but the flexural cracks in the constant moment region widened. The failure of a control beam is shown in Fig 12.

Fig. 12. Flexural failure for control beam.

3.1.2 Retrofitted Beams

The load–deflection curves for the individual beams in series RF1, RF2 and RF3 are shown in Fig. 13. The results from the two nominally equal beams in each series are close, which indicates that the retrofitting was performed in a well-defined manner. The mean curve will be used in the following.

The mean load–deflection curves for the retrofitted beams and for the control beams are shown in Fig. 14. As shown in the figure the stiffness of all beams at small load is almost the same. From a load around 60 kN -cracking stage- the stiffness of the control beam decreases notably due to cracking. The decrease in stiffness is smaller for the retrofitted beams since the CFRP prevents cracks to develop and widen. The longer the CFRP the stiffer the beam. This is probably because the longer CFRP strips have a full anchorage length outside the maximum moment region and are hence more efficient in the cracking zone. Some contribution to the stiffness may also be due to the stiffening of the beam caused by the CFRP outside the cracking region.

It should be noted that if a control beam would be loaded until cracking, unloaded, and then subjected to load again, the stiffness would be somewhat lower the second time due to the damage in the beam. This means that even if the curve of series RF3 is similar to that of the control beam the CFRP has improved the beam and restored the stiffness to the level of the control beam.

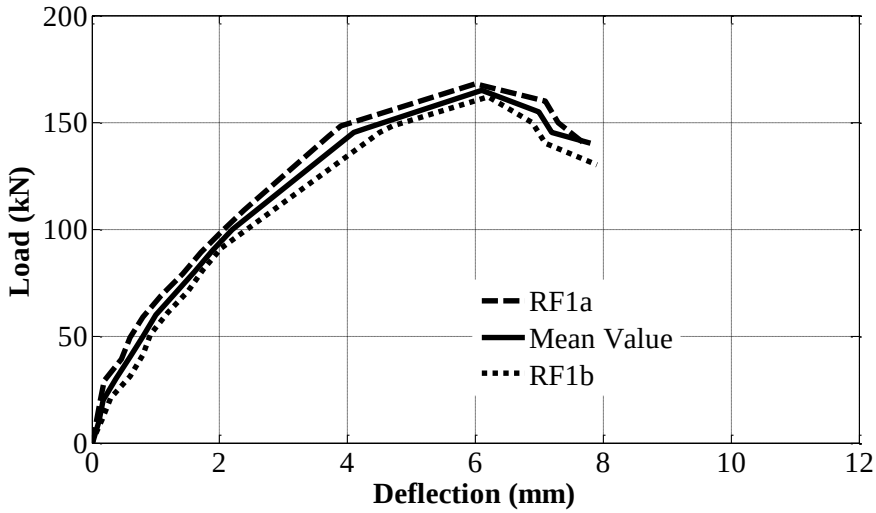
200
150
100
50
0
Load (kN)
0
2
4
6
8
10
12
Deflection (mm)
RF1a
Mean Value
RF1b

(a)

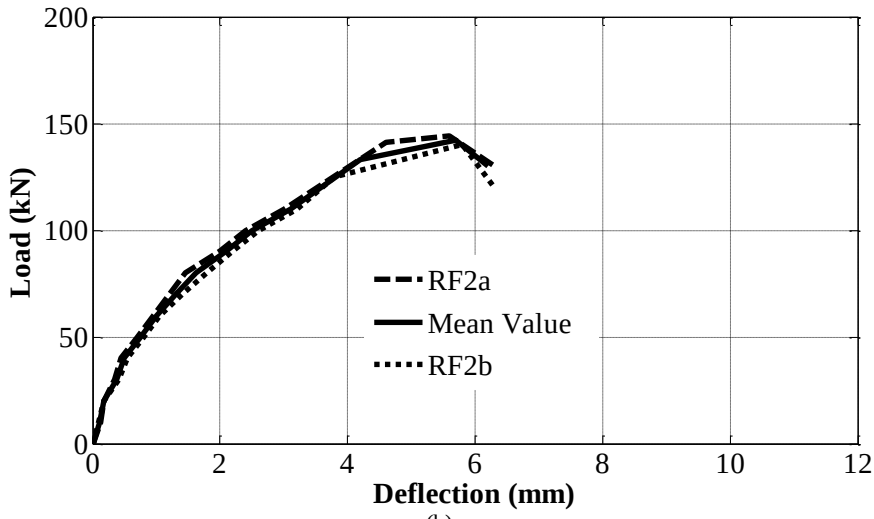
200
150
100
50
0
Load (kN)
0
2
4
6
8
10
12
Deflection (mm)
RF2a
Mean Value
RF2b

(b)

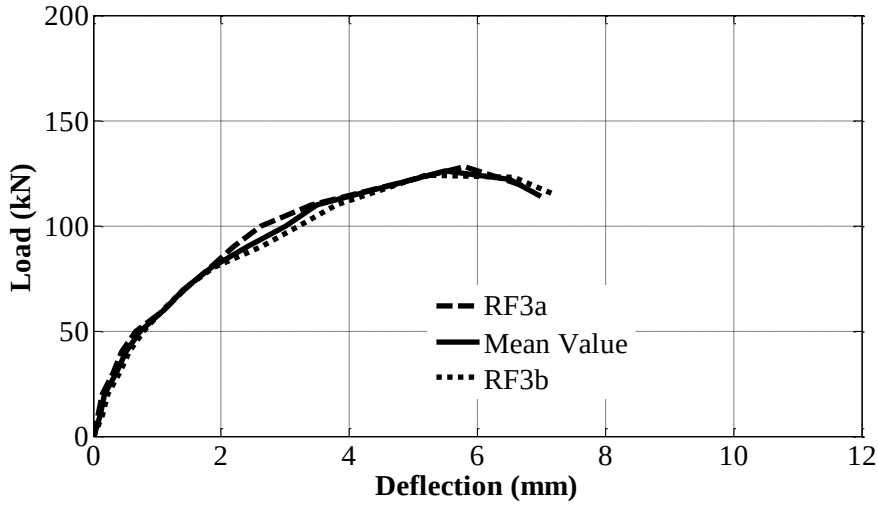

(c)

Fig. 13. Comparison between load-deflection curves for individual retrofitted beams in group RF. (a) series RF1, (b) series RF2 and (c) series RF3.

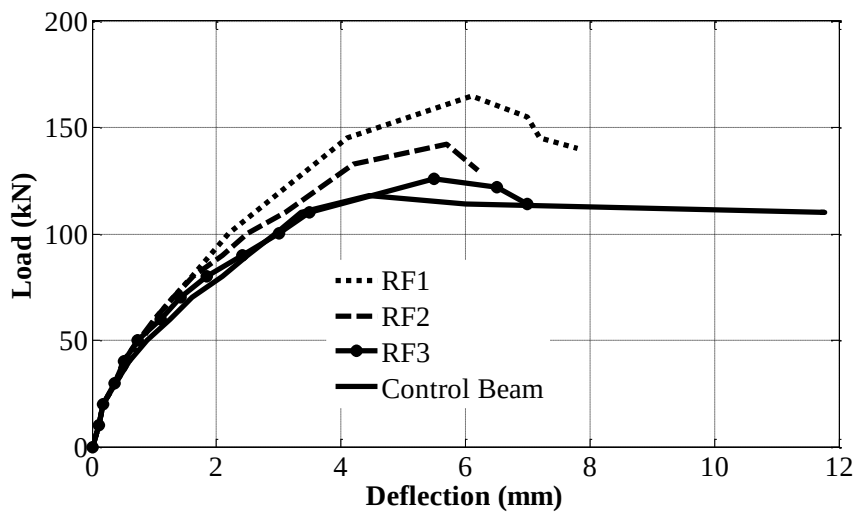

Fig. 14. Comparison between mean load-deflection curves for retrofitted beams and control beam in group RF.

The curves reveal that the strengthening process has significantly increased the maximum load in series RF1 and RF2. The maximum load in series RF1 was 166 kN, which is a more than 33 % increase compared to the control beam. The maximum load for series RF2 was 142 kN, 20 % higher than for the control beam. For series RF3 the maximum load was 128 kN which corresponds to a 7 % increase in maximum load.

All beams experienced a brittle failure mechanism, however in this case sudden debonding of the CFRP plate from the concrete occurred without concrete splitting. This failure was due to high shear stress occurring at the ends of the CFR. The properties of the adhesive are probably important in relation to the debonding failure. A lower stiffness and higher fracture energy will probably weaken the tendency of debonding. For RF2 and RF3 debonding occurred earlier than for RF1. The main reason leading to this is that RF2 and RF3 do not have a full anchorage length outside the maximum moment region, hence higher shear stress concentration will occur compared to for the longest CFRP, Fig. 15. The crack propagation and the final crack pattern of the beam are greatly different from that of the control beam. The control beam had few flexural cracks with large width, and the retrofitted beam had many flexural cracks with smaller width. This indicates that the propagation of cracks was confined by the CFRP laminates. In addition, the cracks in series RF1 were fewer and had smaller width than in the other retrofitted beams.

Fig. 15. Debonding failures in group RF.

The results indicate that the externally bonded CFRP has increased the stiffness and maximum load of the beam. In addition, the crack width and the deflection have decreased. The efficiency of the strengthening by CFRP in flexure varied depending on the length of the CFRP.

3.2 Beams in group RS

3.2 1 Control Beam

The load versus midspan deflection curves for the control beams are shown in Fig. 16. It is clear that the beam failed in a brittle manner and has a low energy absorption before failure.

This is the typical behaviour of an ordinary RC member with insufficient shear steel [15]. The difference between the two specimens is rather small, and the mean value, also indicated in the figure, will be used.

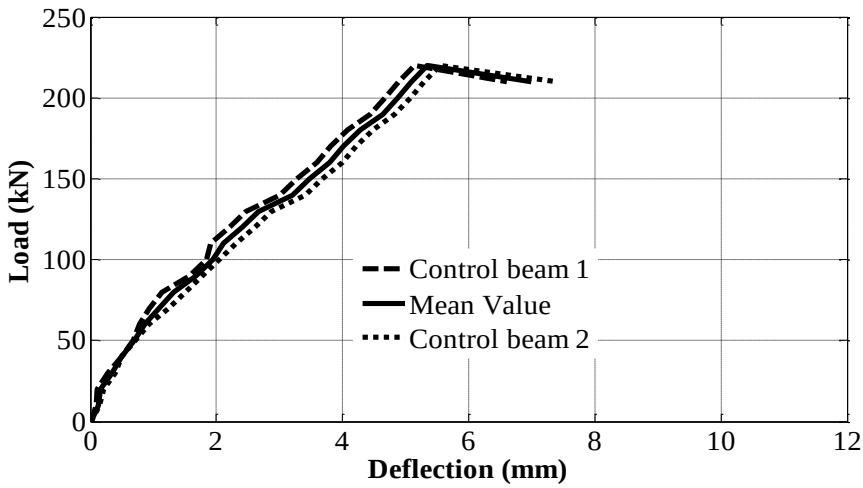

Fig. 16. Comparison between load-deflection curves for individual control beams in group RS.

The curve has linear response until 60 kN. The ultimate load of the control beams was 220 kN. The cracking patterns consist of a pure diagonal shear crack in the constant shear spans, Fig. 17. This is due to the reduced amount of shear reinforcement.

Fig. 17. Shear failure for control beam.

3.2.2 Retrofitted beams

A debonding failure occurred for all beams also in this group. The debonding mode is due to cracking of the concrete underneath the CFRP plate. The beam after failure appears in Fig. 18, which clearly shows the shear crack cross the bond area in the concrete.

The load-deflection curves for the two beams and the mean value are shown in Fig.19. Also here, the variation between the individual beams was small.

The load versus midspan deflection curve for the mean value of the retrofitted beams is compared with the response of the control beams in Fig. 20.

The control beam shows more softening due to crack propagation, while in the retrofitted beam, the cracks are arrested by the CFRP, and this makes the curve of the retrofitted beam somewhat straighter than the control beam curve. The maximum load of the strengthened beam was 270 kN. It may be observed that strengthening increases the maximum load by over 23 %, when compared with the control beam.

Fig. 18. Debonding and shear failures in group RS.

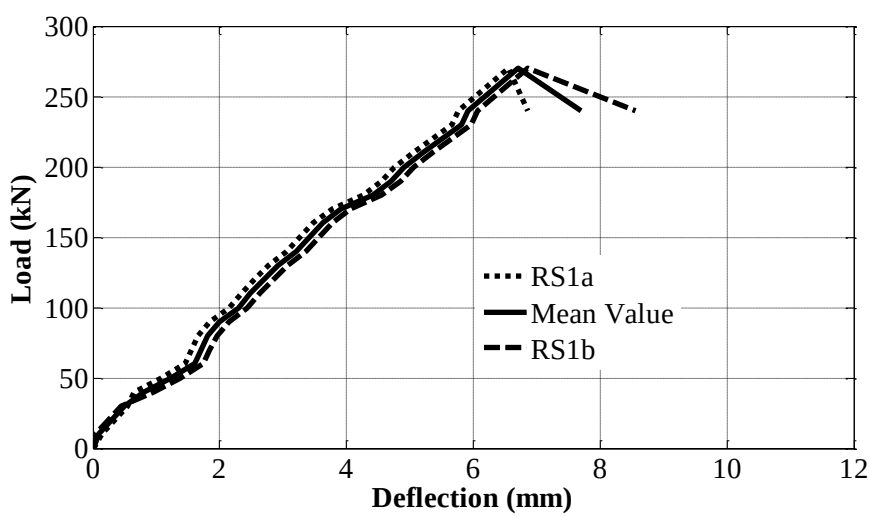

Fig. 19. Comparison between load-deflection curves for individual retrofitted beams in group RS.

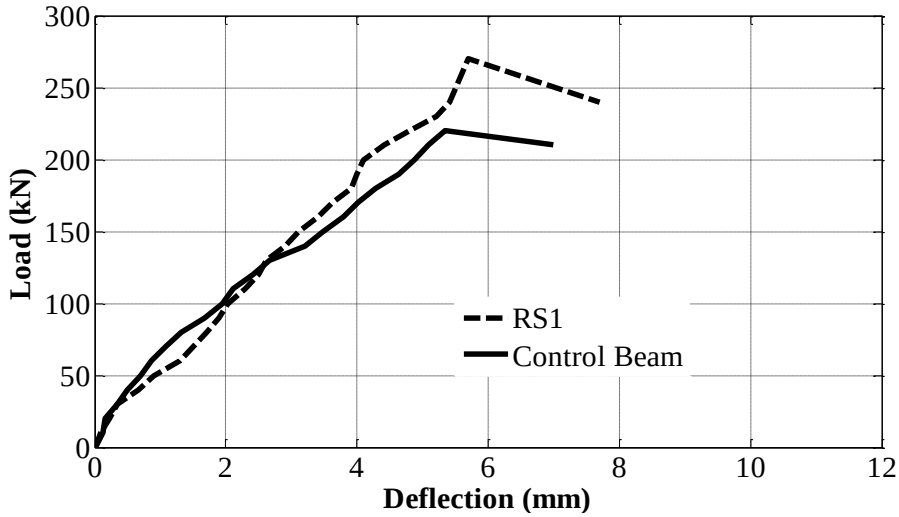

Fig. 20. Comparison between mean load-deflection curves for retrofitted beams and control beam in group RS.

4. Concluding and remarks

The paper investigated the flexural and shear behaviour of reinforced beams retrofitted with CFRP after preloading. The following conclusions are drawn from this experimental study:

- The stiffness of the CFRP-retrofitted beams is increased compared to that of the control beams.
- Employing externally bonded CFRP plates resulted in an increase in maximum load. The increase in maximum load of the retrofitted specimens reached values of about 23 % for retrofitting in shear and between 7% and 33 % for retrofitting in flexure. Moreover, retrofitting shifts the mode of failure to be brittle.
- The crack width for the retrofitted beams is decreased compared to the control beams.
- Experimental results showed that increasing the CFRP plate length in flexural retrofitting can make the CFRP more effective for concrete repair and strengthening. This means that insufficient strengthening lengths do not produce the intended strengthening effect.
- The results showed that the main failure mode was plate debonding which reduces the efficiency of retrofitting.

Based on this conclusion deeper studies should be performed to investigate the behaviour of the interface layer between the CFRP and concrete. Also numerical work should be done to predict the behaviour of retrofitted beams and to evaluate the influence of different parameters on the overall behaviour of the beams.

5. References

[1] Toutanji, H., Zhao, L., and Zhang, Y., "Flexural behaviour of reinforced concrete beams externally strengthened with CFRP sheets bonded with an inorganic matrix". Engineering Structures March 2006; 28: 557-566.

[2] Kachlakev D., McCurry D.D. "Behavior of full-scale reinforced concrete beams retrofitted for shear and flexural with FRP laminates", Composites 2000; 31: 445-452.

[3] David, E, Djelal, C, and Buyle-Bodin, F. "Repair And Strengthening Of Reinforced Concrete Beams Using Composite Materials", 2nd Int. PhD Symposium in Civil Engineering 1998 Budapest.

[4] Shahawy M. A., Arockiasamy T M., Beitelmant T., and Sowrirajan R. "Reinforced concrete rectangular beams strengthened with CFRP laminates", Composites: 1996; 27: 225-233.

[5] Khalifa A, Nanni A . "Rehabilitation of rectangular simply supported RC beams with shear deficiencies using CFRP composites". Construction and Building Materials 2002; 16:135-146.

[6] Shehata, A.E.M, Cerqueira, E.C.,Pinto, C.T.M., and Coppe, "Strengthening of R.C beams in flexure and shear using CFRP laminate.", Fiber-reinforced Plastic for Reinforced Concrete Structure 2001; 1: 97-106.

[7] Khalifa, A., Tumialan, G., Nanni, A. and Belarbi, A., "Shear Strengthening of Continuous RC Beams Using Externally Bonded CFRP Sheets,", American Concrete Institute, Proc., 4th International Symposium on FRP for Reinforcement of Concrete Structures (FRPRCS4), Baltimore, MD, Nov. 1999: 995-1008.

[8] Ferreira, A. J. M. "On the shear-deformation theories for the analysis of concrete shells reinforced with external composite laminates", Strength of Materials 2003; 35(2): 128-135

[9] Karunasena, W., Hardeo, P., Bosnich, G. Rehabilitation of concrete beams by externally bonding fiber composite reinforcement. In Composite Systems: Macrocomposites, Microcomposites, Nanocomposites, Proceedings of the ACUN-4, International Composites Conference, 4th, Sydney, Australia July 21-25, 2002; 222-226.

[10] ASTM C136. Method of seive analysis of fine and coarse aggregate, ASTM International.

[11] ACI Comitte 211.1-91. Standard practice for selecting proportion for normal, heavy weight and mass concrete. ACI Manual of Concrete Practice. Part 1, 1996.

[12] http: \\ www.fosroc.com. 2009, Dec, 16.

[13] ACI Comittee 318. Building Code Requirements for Structural Concrete and Commentary (ACI 318-99). American Concrete Institute Detroit, MI, 1999.

[14] Nilson, H., Darwin, D., and Dolan, C.W. Design of Concrete structures, 13th edition.. McGraw Hill Higher Education, 2004.

[15] Nielsen, M. P.: Limit analysis and concrete plasticity, second edition, CRC press, 1999.
[16] Obaidat,Y. Retrofitting of reinforced concrete beams using composite laminates, Master Thesis, Jordan University of Science and Technology. 2007.

Paper B

B

The effect of CFRP and CFRP/ concrete interface models when modelling retrofitted RC beams with FEM.

Yasmeen Taleb Obaidat, Susanne Heyden and Ola Dahlblom

Published in Composite Structures, 2010; 92: 1391–1398.

Composite Structures 92 (2010) 1391–1398

Contents lists available at ScienceDirect

Composite Structures

journal homepage: www.elsevier.com/locate/compstruct

The effect of CFRP and CFRP/concrete interface models when modelling retrofitted RC beams with FEM

Yasmeen Taleb Obaidat *, Susanne Heyden, Ola Dahlblom

Division of Structural Mechanics, Lund University, Lund, Sweden

ARTICLE INFO

Article history:
Available online 14 November 2009

Keywords:
Carbon fibre reinforced plastic (CFRP)
Strengthening
Laminate
Cohesive model
Reinforced concrete beam
Finite element analysis (FEA)

ABSTRACT

Concrete structures retrofitted with fibre reinforced plastic (FRP) applications have become widespread in the last decade due to the economic benefit from it. This paper presents a finite element analysis which is validated against laboratory tests of eight beams. All beams had the same rectangular cross-section geometry and were loaded under four point bending, but differed in the length of the carbon fibre reinforced plastic (CFRP) plate. The commercial numerical analysis tool Abaqus was used, and different material models were evaluated with respect to their ability to describe the behaviour of the beams. Linear elastic isotropic and orthotropic models were used for the CFRP and a perfect bond model and a cohesive bond model was used for the concrete–CFRP interface. A plastic damage model was used for the concrete. The analyses results show good agreement with the experimental data regarding load–displacement response, crack pattern and debonding failure mode when the cohesive bond model is used. The perfect bond model failed to capture the softening behaviour of the beams. There is no significant difference between the elastic isotropic and orthotropic models for the CFRP.

1. Introduction

Upgrading of reinforced concrete structures may be required for many different reasons. The concrete may have become structurally inadequate for example, due to deterioration of materials, poor initial design and/or construction, lack of maintenance, upgrading of design loads or accident events such as earthquakes. In recent years, the development of strong epoxy glue has led to a technique which has great potential in the field of upgrading structures. Basically the technique involves gluing steel or FRP plates to the surface of the concrete. The plates then act compositely with the concrete and help to carry the loads.

The use of FRP to repair and rehabilitate damaged steel and concrete structures has become increasingly attractive due to the well-known good mechanical properties of this material, with particular reference to its very high strength to density ratio. Other advantages are corrosion resistance, reduced maintenance costs and faster installation time compared to conventional materials.

The application of CFRP as external reinforcement to strengthen concrete beams has received much attention from researchers [1–5], but only very few studies have focused on structural members strengthened after preloading [6,7]. The behaviour of structures which have been preloaded until cracking initiates deserves more attention, since this corresponds to the real-life use of CFRP retrofitting.

Researchers have observed new types of failures that can reduce the performance of CFRP when used in retrofitting structures [8]. These failures are often brittle, and include debonding of concrete layers, delamination of CFRP and shear collapse. Brittle debonding has particularly been observed at laminate ends, due to high concentration of shear stresses at discontinuities, where shear cracks in the concrete are likely to develop [9]. Thus, it is necessary to study and understand the behaviour of CFRP strengthened reinforced concrete members, including those failures.

Several researchers have simulated the behaviour of the concrete–CFRP interface through using a very fine mesh to simulate the adhesive layer defined as a linear elastic material [10]. However, they have not used any failure criterion for the adhesive layer. Most researchers who have studied the behaviour of retrofitted structures have, however, not considered the effect of the interfacial behaviour at all [11–13].

In this paper, we use the finite element method to model the behaviour of beams strengthened with CFRP. For validation, the study was carried out using a series of beams that had been experimentally tested for flexural behaviour and reported by Obaidat [14]. Two different models for the CFRP and two different models for the concrete–CFRP interface are investigated. The models are used for analysing beams with different lengths of CFRP applied.

* Corresponding author.
E-mail address: Yasmeen.Obaidat@byggmek.lth.se (Y.T. Obaidat).

0263-8223/$ - see front matter © 2009 Elsevier Ltd. All rights reserved.
doi:10.1016/j.compstruct.2009.11.008

2. Experimental work

Experimental data was obtained from previous work by Obaidat [14]. Eight identical RC beams were loaded with a four point bending configuration with a span of 1560 mm, and distance between loads of 520 mm. All beams were 300-mm high, 150-mm wide, and 1960-mm long. The longitudinal reinforcement consisted of two ϕ 12 for tension and two ϕ 10 for compression. Shear reinforcement was sufficiently provided and consisted of ϕ 8 c/c 100 mm, as seen in Fig. 1.

Two control beams were loaded to failure and the other beams were loaded until cracks appeared, then retrofitted using different lengths of CFRP, see Fig. 2. The CFRP was adhered to the bottom surface of the beams with their fibre direction oriented in the axial direction of the beam. Each CFRP plate was 1.2 mm thick and 50 mm wide. Finally the beams were retested, while the deflection and load were monitored.

A comparison of load–deflection curves of retrofitted beams and control beams is presented in Fig. 3. The experimental results showed that the retrofitting using CFRP increased the strength of the beam and the effect increased with the length of the CFRP plate. All retrofitted beams failed due to debonding of the CFRP.

3. Finite element analysis

Finite element failure analysis was performed to model the nonlinear behaviour of the beams. The FEM package Abaqus/standard [15] was used for the analysis.

3.1. Material properties and constitutive models

3.1.1. Concrete

A plastic damage model was used to model the concrete behaviour. This model assumes that the main two failure modes are tensile cracking and compressive crushing [15]. Under uni-axial tension the stress–strain response follows a linear elastic relationship until the value of the failure stress is reached. The failure stress corresponds to the onset of micro-cracking in the concrete material. Beyond the failure stress the formation of micro-cracks is represented with a softening stress–strain response. Hence, the elastic parameters required to establish the first part of the relation are elastic modulus, E_c, and tensile strength, f_{ct}, Fig. 4a. The compressive strength, f'_c, was in the experimental work measured to be 30 MPa. E_c and f_{ct} were then calculated by [16]:

$$E_c = 4700\sqrt{f'_c} = 26{,}000 \text{ MPa} \quad (1)$$

$$f_{ct} = 0.33\sqrt{f'_c} = 1.81 \text{ MPa} \quad (2)$$

where f'_c, is given in MPa.

To specify the post-peak tension failure behaviour of concrete the fracture energy method was used. The fracture energy for mode I, G_f, is the area under the softening curve and was assumed equal to 90 J/m^2, see Fig. 4b.

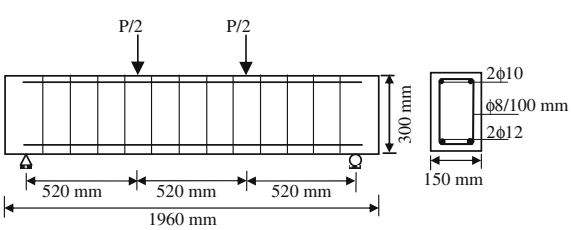

Fig. 1. Geometry, reinforcement and load of the tested beams.

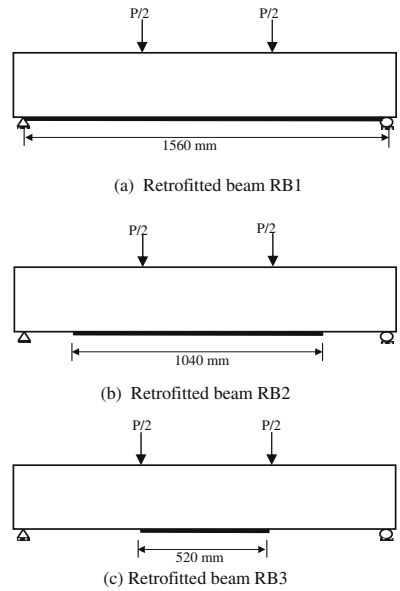

Fig. 2. Length of CFRP laminates in test series RB1, RB2 and RB3.

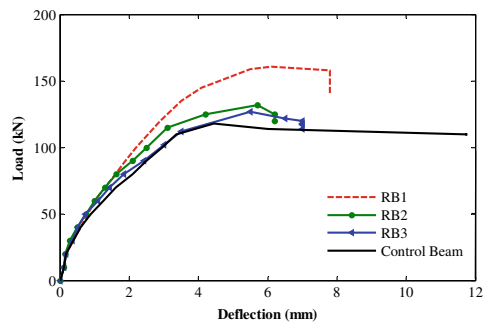

Fig. 3. Load versus mid-span deflection for un-strengthened and strengthened beams.

The stress–strain relationship proposed by Saenz [17] was used to construct the uni-axial compressive stress–strain curve for concrete:

$$\sigma_c = \frac{E_c \varepsilon_c}{1 + (R + R_E - 2)\left(\frac{\varepsilon_c}{\varepsilon_0}\right) - (2R - 1)\left(\frac{\varepsilon_c}{\varepsilon_0}\right)^2 + R\left(\frac{\varepsilon_c}{\varepsilon_0}\right)^3} \quad (3)$$

where

$$R = \frac{R_E(R_\sigma - 1)}{(R_\varepsilon - 1)^2} - \frac{1}{R_\varepsilon}, \quad R_E = \frac{E_c}{E_0}, \quad E_0 = \frac{f'_c}{\varepsilon_0} \quad (4)$$

and, $\varepsilon_0 = 0.0025$, $R_\varepsilon = 4$, $R_\sigma = 4$ as reported in [18]. The stress–strain relationship in compression for concrete is represented in Fig. 5.

Poisson's ratio for concrete was assumed to be 0.2.

3.1.2. Steel reinforcement

The steel was assumed to be an elastic–perfectly plastic material and identical in tension and compression as shown in Fig. 6.

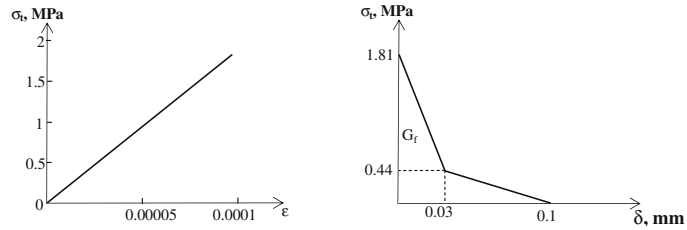

(a) Stress-strain relationship up to ultimate load. (b) Post-peak stress deformation relationship.

Fig. 4. Concrete under uni-axial tension.

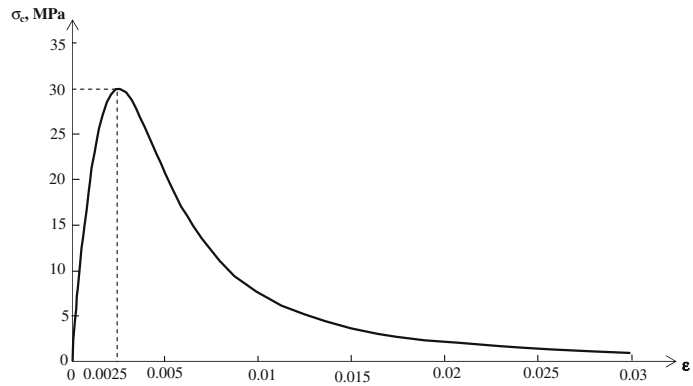

Fig. 5. Stress–strain relationship for concrete under uni-axial compression.

The elastic modulus, E_s, and yield stress, f_y, were measured in the experimental study and the values obtained were $E_s = 209$ GPa and $f_y = 507$ MPa. These values were used in the FEM model. A Poisson's ratio of 0.3 was used for the steel reinforcement. The bond between steel reinforcement and concrete was assumed as a perfect bond.

3.1.3. CFRP

Two different models for the CFRP were used in this study. In the first model, the CFRP material was considered as linear elastic isotropic until failure. In the second model, the CFRP was modelled as a linear elastic orthotropic material. Since the composite is unidirectional it is obvious that the behaviour is essentially orthotropic. In a case like this however, where the composite is primarily stressed in the fibre direction, it is probable that the modulus in the fibre direction is the more important parameter. This is why an isotropic model is considered suitable. The elastic modulus in the fibre direction of the unidirectional CFRP material used in the experimental study was specified by the manufacturer as 165 GPa. This value for E and $v = 0.3$ was used for the isotropic model. For the orthotropic material model E_{11} was set to 165 GPa. Using Rule of Mixture [19], $E_{epoxy} = 2.5$ GPa and that the fibre volume fraction was 75%, E_{fibre} was found to be 219 GPa and $v_{12} = v_{13} = 0.3$. By use of Inverse Rule of Mixture [19], $E_{22} = E_{33} = 9.65$ GPa and $G_{12} = G_{13} = 5.2$ GPa. v_{23} and G_{23} were set to 0.45 and 3.4, respectively.

3.1.4. CFRP–concrete interface

Two different models were used to represent the interface between concrete and CFRP. In the first model the interface was modelled as a perfect bond while in the second it was modelled using a cohesive zone model. Fig. 7 shows a graphic interpretation of a simple bilinear traction–separation law written in terms of the effective traction τ and effective opening displacement δ. The interface is modelled as a rich zone of small thickness and the initial stiffness K_0 is defined as [20]:

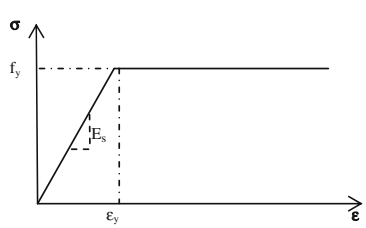

Fig. 6. Stress strain behaviour of steel.

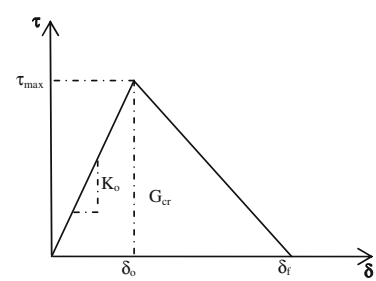

Fig. 7. Bilinear traction–separation constitutive law.

$$K_0 = \frac{1}{\frac{t_i}{G_i} + \frac{t_c}{G_c}} \quad (5)$$

where t_i is the resin thickness, t_c is the concrete thickness, and G_i and G_c are the shear modulus of resin and concrete respectively. The values used for this study were $t_i = 1$ mm, $t_c = 5$ mm, $G_i = 0.665$ GPa, and $G_c = 10.8$ GPa.

From Fig. 7, it is obvious that the relationship between the traction stress and effective opening displacement is defined by the stiffness, K_0, the local strength of the material, τ_{max}, a characteristic opening displacement at fracture, δ_f, and the energy needed for opening the crack, G_{cr}, which is equal to the area under the traction–displacement curve. Eq. (6), [21], provides an upper limit for the maximum shear stress, τ_{max}, giving $\tau_{max} = 3$ MPa in this case:

$$\tau_{max} = 1.5\beta_w f_t \quad (6)$$

where

$$\beta_w = \sqrt{\left(2.25 - \frac{b_f}{b_c}\right) \Big/ \left(1.25 + \frac{b_f}{b_c}\right)}$$

and b_f is CFRP plate width, b_c is concrete width and f_{ct} is concrete tensile strength.

Numerical simulations showed that this value is too high; since CFRP rupture or concrete crushing induced the failure, instead of the CFRP debonding that occurred in the experimental study, see Fig. 8. The two curves representing $\tau_{max} = 3$ MPa show increasing load up to failure, and the simulations ended with CFRP rupture or concrete crushing. Hence, τ_{max} was reduced to 1.5 MPa.

For fracture energy, G_{cr}, previous researches have indicated values from 300 J/m^2 up to 1500 J/m^2 [22,23]. To investigate to what extent G_{cr} affects the results, numerical simulations were performed for $G_{cr} = 500$ J/m^2 and 900 J/m^2. The simulations showed that G_{cr} has in this case only a moderate influence on the load–deformation behaviour, as seen in Fig. 8. For this study the value 900 J/m^2, in the middle of the interval proposed by previous studies, was used.

The initiation of damage was assumed to occur when a quadratic traction function involving the nominal stress ratios reached the value one. This criterion can be represented by [15]:

$$\left\{\frac{\sigma_n}{\sigma_n^0}\right\}^2 + \left\{\frac{\tau_n}{\tau_s^0}\right\}^2 + \left\{\frac{\tau_t}{\tau_t^0}\right\}^2 = 1 \quad (7)$$

where σ_n is the cohesive tensile and τ_s and τ_t are shear stresses of the interface, and n, s, and t refer to the direction of the stress component, see Fig. 9b. The values used for this study were $\sigma_n^0 = f_{ct} = 1.81$ MPa, and $\tau_s^0 = \tau_t^0 = 1.5$ MPa.

Interface damage evolution was expressed in terms of energy release. The description of this model is available in the Abaqus material library [15]. The dependence of the fracture energy on the mode mix was defined based on the Benzaggah–Kenane fracture criterion [15]. Benzaggah–Kenane fracture criterion is particularly useful when the critical fracture energies during deformation purely along the first and the second shear directions are the same; i.e., $G_s^C = G_t^C$. It is given by:

$$G_n^C + \left(G_s^C - G_n^C\right)\left\{\frac{G_{\mathscr{S}}}{G_{\mathscr{T}}}\right\}^{\eta} = G^C \quad (8)$$

where $G_{\mathscr{S}} = G_S + G_t$, $G_{\mathscr{T}} = G_n + G_s$, and η are the material parameter. G_n, G_s and G_t refer to the work done by the traction and its conjugate separation in the normal, the first and the second shear directions, respectively. The values used for this study were $G_n^C = 90$ J/m^2, $G_t^C = G_s^C = 900$ J/m^2, and $\eta = 1.45$.

3.2. Numerical analysis

4-Node linear tetrahedral elements were used for the reinforced concrete, reinforcement steel, steel plates at supports and under the load, and CFRP in this model. The element configuration is shown in Fig. 9a. 8-Node 3-D cohesive elements were used to model the interface layer. The cohesive interface elements are composed of two surfaces separated by a thickness, Fig. 9b. The relative motion of the bottom and top parts of the cohesive element measured along the thickness direction represents opening or closing of the interface. The relative motion of these parts represents the transverse shear behaviour of the cohesive element.

To show the effect of the bond model and the behaviour of CFRP, four combinations of bond model and CFRP model were analysed; Perfect bond with isotropic CFRP, perfect bond with orthotropic CFRP, cohesive bond model with isotropic CFRP, and cohesive bond model with orthotropic CFRP.

One quarter of the specimen was modelled, as shown in Fig. 10, by taking advantage of the double symmetry of the beam. The boundary conditions are illustrated in Fig.11. A fine mesh is needed to obtain results of sufficient accuracy. The pre-crack was modelled by making a gap of 0.1 mm width and 10 mm depth between the continuum elements, 20 mm from the centre of the beam. Table 1 shows the number of elements, number of degrees of freedom and CPU time. The processor type used for this study was 2 Xeon 5160 (3.0 GHz, dual core).

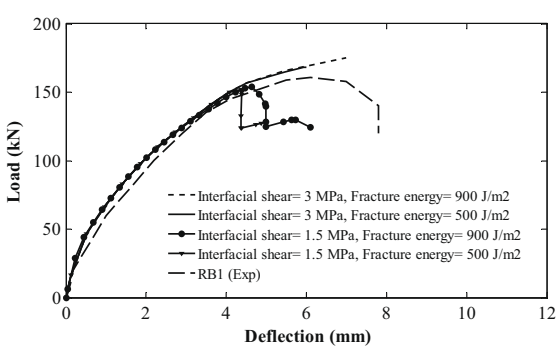

Fig. 8. Comparison between the experimental and the FE analysis results for different model of interfacial behaviour and isotropic behaviour for CFRP for beam RB1.

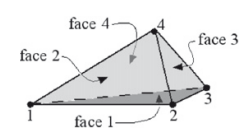

(a) 4-node linear tetrahedral element.

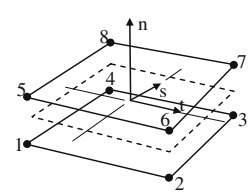

(b) 8-node 3-D cohesive element.

Fig. 9. Elements used in the numerical analysis.

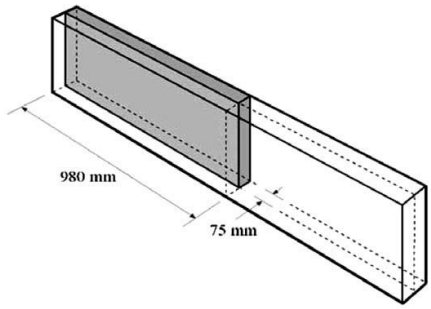

(a) By use of symmetry, one quarter of the beam was modelled.

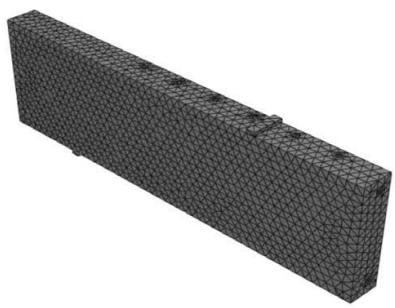

(b) Finite element mesh of quarter of beam.

Fig. 10. Geometry and elements used in the numerical analysis.

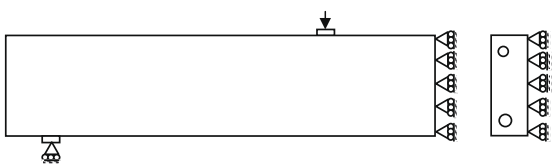

Fig. 11. Boundary conditions used in numerical work.

Table 1
Model size and computational time.

Model	Number of elements	Number of degrees of freedom (DOF)	CPU time (h)
Control beam	150,813	79,428	2:54
Isotropic CFRP/ perfect bond			
RB1	168,630	89,595	3:41
RB2	169,019	89,583	4:25
RB3	168,917	89,406	4:05
Orthotropic CFRP/ perfect bond			
RB1	168,630	89,595	6:36
RB2	169,019	89,583	2:57
RB3	168,917	89,406	2:40
Isotropic CFRP/ cohesive model			
RB1	168,669	90,075	4:06
RB2	169,656	90,189	3:08
RB3	170,307	90,240	2:30
Orthotropic CFRP/ cohesive model			
RB1	168,669	90,075	3:41
RB2	169,656	90,189	2:50
RB3	170,307	90,240	2:52

3.3. Nonlinear solution

In this study the total deflection applied was divided into a series of deflection increments. Newton method iterations provide convergence, within tolerance limits, at the end of each deflection increment. During concrete cracking, steel yielding and the ultimate stage where a large number of cracks occur, the deflections are applied with gradually smaller increments. Automatic stabilization and small time increment were also used to avoid a diverged solution.

4. Results

4.1. Load–deflection curves

The load–deflection curves obtained for control beam and retrofitted beams from experiments and FEM analysis are shown in Fig. 12. Four different combinations of models for CFRP and concrete/CFRP bond were used.

There is good agreement between FEM and experimental results for the control beam, Fig. 12a. The FEM analysis predicts the beam to be slightly stiffer and stronger, probably because of the assumed perfect bond between concrete and reinforcement. The good agreement indicates that the constitutive models used for concrete and reinforcement can capture the fracture behaviour well.

When comparing Fig. 12a–d, it can be seen that the length of the CFRP significantly influences the behaviour of the beam. The longer CFRP, the higher is the maximum load.

For the retrofitted beams, the results from the four different FEM models are close to identical during the first part of the curve, all slightly stiffer than the experimental results, Fig. 12b–d.

After cracks start appearing, the perfect bond models increasingly overestimate the stiffness of the beam. This is due to the fact that the perfect bond does not take the shear strain between the concrete and CFRP into consideration. This shear strain increases when cracks appear and causes the beam to become less stiff.

The perfect bond models also fail to capture the softening of the beam, a fact that is most obvious for RB1. Debonding failure, which occurred in the experiments, is not possible with the perfect bond model. Thus, it is possible to increase the load further until another mode of failure occurs. In this case shear flexural crack failure or CFRP rupture. The curves for isotropic and orthotropic perfect bond models are close to coincident, but the orthotropic perfect bond model gives a maximum load value that is slightly smaller than the isotropic perfect bond model. This is possibly because the unrealistically high stiffness in the transverse direction and shear of the isotropic CFRP provides a strengthening confinement.

The cohesive models show good agreement with the experimental results. There are only small differences between the isotropic and orthotropic cohesive models.

There are several possible causes for the differences between the experimental data and the finite element analysis. One is, as for the control beam, the assumed perfect bond between concrete and steel reinforcement. In addition, the location and dimensions of the pre-crack were not represented exactly as it appeared in the experimental work; another reason is due to the estimation of the behaviour of the interface between CFRP and concrete. This may lead to the overestimation of the stiffness and capacity of the reinforced concrete structural element.

The results show that a cohesive model gives good agreement with experimental results, but the perfect bond model does not, at least not for high load levels. The results also show that it is not necessary to take into account the orthotropic properties of the unidirectional CFRP.

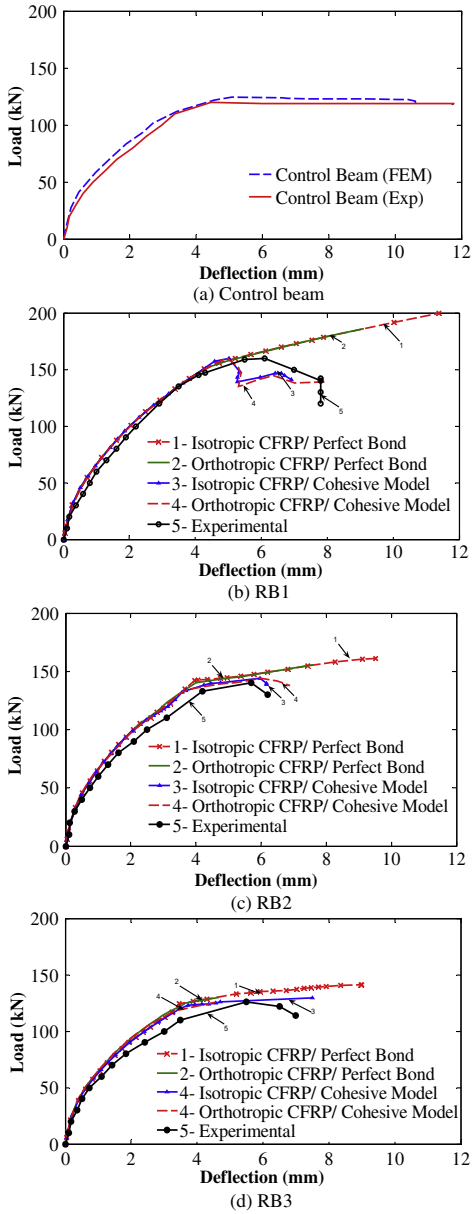

Fig. 12. Load–deflection curves of beams, obtained by experiments and different models.

4.2. Effect of retrofitting on the stress

Fig. 13 shows the differences between the axial stress for the control specimens and the retrofitted beam RB2 at load equal to 10 kN. All models which were used in this study gave the same indication for this point. Also the parts of the strengthened beams a long distance from the CFRP have a different stress distribution compared to those of the un-strengthened specimens at the corresponding location. This indicates that the effect of the strengthening is not local but it affects the stress distribution of the beam as a whole.

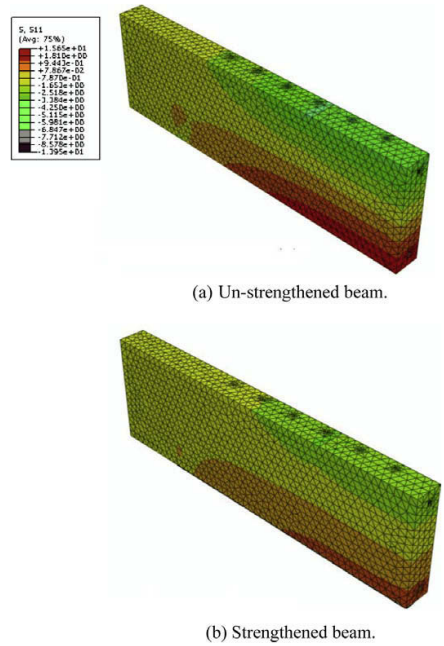

Fig. 13. Comparison of axial stress distribution between un-strengthened beam and strengthened beam, RB2.

4.3. Evolution of cracks

As the concrete damage plasticity model does not have a notation of cracks developing at the material integration point, it was assumed that cracking initiates at the points where the maximum principal plastic strain is positive, following Lubliner et al. [24]. Fig. 14 shows a comparison between plastic strain distributions obtained from the finite element analysis and crack patterns obtained from the experiments for the control beam and strengthened beams. The cracks obtained in the experiments and in the simulations are similar, which indicates that the model can capture the mechanisms of fracture in the beams.

4.4. Failure mode

The perfect bond model does not include fracture of the bond, and is thus unable to model the debonding fracture mode which the experiments showed. The cohesive model, on the other hand, can represent debonding. When the cohesive bond model was used debonding fracture occurred, just like in the experiments. This is illustrated in Fig. 15.

4.5. Stress in bond layer

Debonding of CFRP is likely to initiate at the stress concentration in the bond layer, which occur in the plate end region and around cracks. A simplified illustration of the axial stress in the composite and the corresponding shear stress in the bond layer for a beam with a constant moment and a mid-span crack is shown in Fig. 16. In the anchorage zone the axial stress in the composite is increasing and the axial force is transmitted to the composite through shear stress in the bond layer. In the crack zone axial force cannot be sustained by the beam itself and axial force is thus transmitted to the composite, resulting in shear stress in the bond layer.

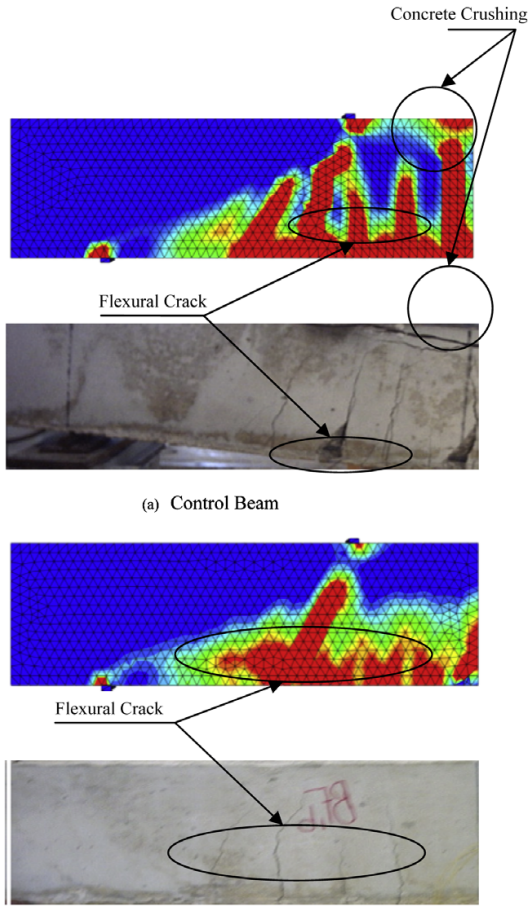

Fig. 14. Comparison between plastic strain distribution from FEM analysis and crack patterns from experiments.

The stress state in the bond layer in the analysed beams is more complicated due to a complex crack pattern and 3-D effects. Still, it is possible to see the phenomena illustrated in Fig. 16.

Fig. 17 illustrates the shear stress in the cohesive layer for RB2 at different load levels. Note that due to symmetry only one half of the beam is represented. From Fig. 17, it can be seen that when the load is equal to 8 kN (i.e., before cracking) there are shear stress concentrations at the pre-cracked region and at the plate end. By increasing the load up to 100 kN (i.e., after the cracks are initiated) the interfacial shear stress increases, and has a maximum value at the plate end. The shear stress also reaches maximum value around the pre-cracked zone due to rapidly transmitted force between the concrete and CFRP. At the ultimate load, 140 kN, debonding has occurred at the plate end, and the maximum shear stress shifts to the mid-span which becomes a new anchorage zone and where the flexural cracks propagate.

Fig. 18 shows the shear stress in the cohesive layer for different CFRP lengths at a load of 100 kN. At this load cracking has initiated. It is clear that when the CFRP length is short, the entire plate is an anchorage zone and the shear stress is high and almost constant, see RB3. For RB1, the anchorage length needed is provided outside the cracking region which leads to an improved performance. Since

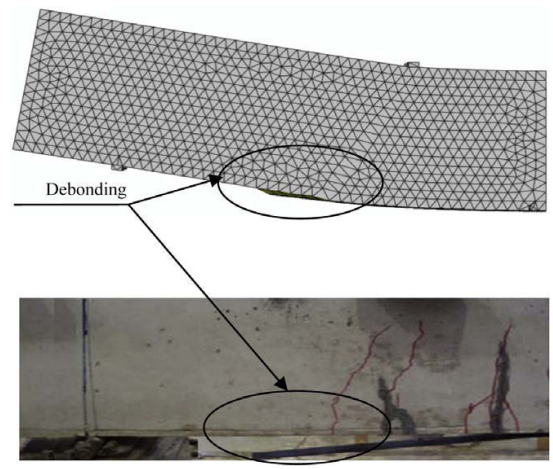

Fig. 15. Comparison of failure mode from FEM analysis and experiment for beam RB2.

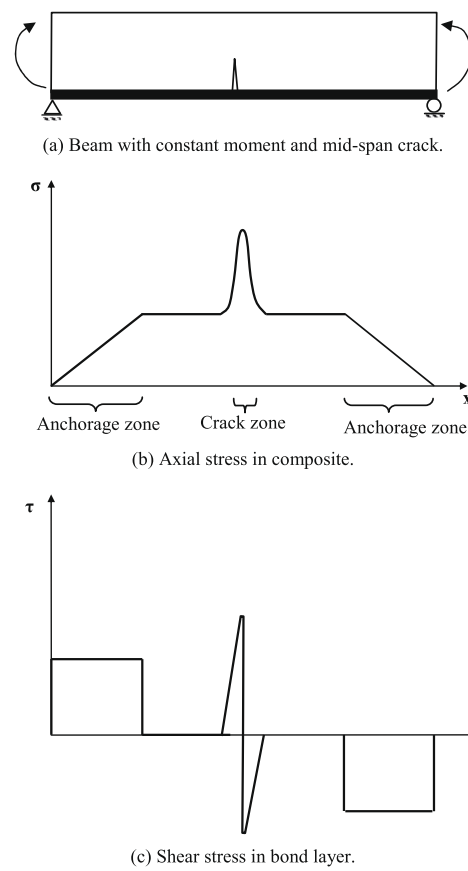

Fig. 16. Axial stress in composite material and shear stress in bond layer.

the moment is decreasing towards the end of the beam, the shear stresses do not reach the same level in the anchorage zone as for RB2 and RB3.

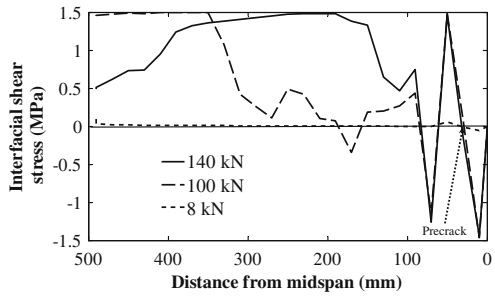

Fig. 17. Shear stress of the interface layer at different loads for beam RB2.

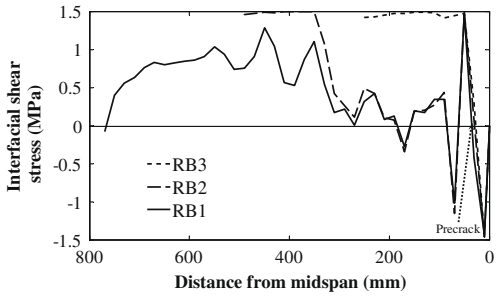

Fig. 18. Shear stress of the interface layer for different beams at 100 kN.

5. Conclusions

A finite element model was developed to analyse beams retrofitted with CFRP. The finite element results show good agreement with the experimental results. Elastic orthotropic and isotropic behaviours were used to represent the CFRP behaviour; also a cohesive model was used to address the interfacial behaviour between CFRP and concrete. The following conclusions can be drawn from this study:

- The behaviour of the retrofitted beams is significantly influenced by the length of CFRP. This is clear in experimental results as well as in numerical analysis. The ultimate load increases with the length of the CFRP.
- The perfect bond model failed to capture the softening of the beams.
- No significant differences were observed when different assumptions were used for CFRP with the cohesive bond model.
- The cohesive model proved able to represent the bond behaviour between CFRP and concrete. The predicted ultimate loads and the debonding failure mode were in excellent correlation with the experimental work.

References

[1] Kachlakev D, Mccurry DD. Behavior of full-scale reinforced concrete beams retrofitted for shear and flexural with FRP laminates. Compos J 2000;31:445–52.
[2] Valivonis J, Skuturna T. Cracking and strength of reinforced concrete structures in flexure strengthened with carbon fibre laminates. Civ Eng Manage J 2006;13(4):317–33.
[3] Yeong-soo S, Chadon L. Flexural behavior of reinforced concrete beams strengthened with carbon fiber-reinforced polymer laminates at different levels of sustaining load. ACI Struct J 2003;100:231–40.
[4] Aram MR, Gzaderski C, Motavalli M. Debonding failure modes of flexural FRP-strengthened RC beam. Compos Part B 2008;39:826–41.
[5] Ashour AF, El-Refaie SA, Garrity SW. Flexural strengthening of RC continuous beams using CFRP laminates. Cement Concr Compos 2004;26:765–75.
[6] Ai-hui Z, Wei-Liang J, Gui-bing L. Behaviour of preloaded RC beams strengthened with CFRP laminates. J Zhejiang Univ Sci A 2006:436–44.
[7] Wenwei W, Guo L. Experimental study of RC beams strengthened with CFRP sheets under sustaining loads. Wuhan Univ Technol – Mater Sci Ed J 2006;21(3).
[8] Esfahani M, Kianoush M, Tajari A. Flexural behaviour of reinforced concrete beams strengthened by CFRP sheets. Eng Struct 2007;29:2428–44.
[9] Teng JG, Smith ST, Yao J, Chen JF. Intermediate crack-introduced debonding in beams and slabs. Construct Build Mater J 2003;17(6–7):447–62.
[10] Ebead U, Marzouk H. Tension–stiffening model for FRP strengthened RC concrete two-way slab. Mater Struct 2004:193–200.
[11] Hu H-T, Lin F-M, Jan Y-Y. Nonlinear finite element analysis of reinforced concrete beams strengthened by fibre-reinforced plastic. Compos Struct J 2004;63:271–81.
[12] Lundquist J, Nordin H, Täljsten B, Olafsson T. Numerical analysis of concrete beams strengthened with CFRP – a study of anchorage lengths. In: FRP in construction, Proceeding of the international symposium of bond behaviour of FRP in structures; 2005. p. 247–54.
[13] Santhakumar R, Chandrasekaran E. Analysis of retrofitted reinforced concrete shear beams using carbon fibre composite. Electron J Struct Eng 2004;4:66–74.
[14] Obaidat Y. Retrofitting of reinforced concrete beams using composite laminates. Master Thesis, Jordan University of Science and Technology; 2007.
[15] Hibbitt, Karlsson, and Sorensen, Inc. ABAQUS Theory manual, User manual and Example Manual, Version 6.7. Providence, RI; 2000.
[16] ACI Committee 318. Building code requirements for structural concrete and commentary (ACI 318-99). Detroit (MI): American Concrete Institute; 1999.
[17] Saenz, LP. Discussion of "Equation for the stress-strain curve of concrete" by Desayi P, Krishnan S. ACI Journal 1964;61:1229–35.
[18] Hu H-T, Schnobrich WC. Constitutive modelling of concrete by using nonassociated plasticity. J Mater Civil Eng (ASCE) 1989;1(4):199–216.
[19] Piggott M. Load bearing fibre composites. 2nd ed. Boston/Dordrecht/London: Kluwer Academic Publishers; 2002.
[20] Guo ZG, Cao SY, Sun WM, Lin XY. Experimental study on bond stress-slip behaviour between FRP sheets and concrete. In: FRP in construction, proceedings of the international symposium on bond behaviour of FRP in structures; 2005. p. 77–84.
[21] Lu XZ, Ten JG, Ye LP, Jaing JJ. Bond-slip models for FRP sheets/plates bonded to concrete. Eng Struct 2005;24(5):920–37.
[22] JCI. Technical report on continuos fibre reinforced concrete. JCI TC952 on continuos reinforced concrete; 1998. p. 116–24.
[23] JCI. Technical report on retrofit technology for concrete structures. Technical committee on retrofitting technology for concrete structures; 2003. p. 79–97.
[24] Lubliner J, Oliver J, Oller S, Oñate E. A plastic-damage model for concrete. Int J Solids Struct 1989;25:299–329.

Paper C

C

Nonlinear FE modelling of shear behaviour in RC beam retrofitted with CFRP

Yasmeen Taleb Obaidat, Ola Dahlblom and Susanne Heyden

Published in proceedings of Computational Modelling of Concrete Structures (EURO-C 2010), Austria, 2010

Computational Modelling of Concrete Structures – Bićanić et al. (eds)

Nonlinear FE modelling of shear behaviour in RC beam retrofitted with CFRP

Yasmeen Taleb Obaidat, Ola Dahlblom & Susanne Heyden
Division of Structural Mechanics, Lund University, Lund, Sweden

ABSTRACT: A nonlinear 3-D numerical model has been developed using the ABAQUS finite element program, and it was used to examine the shear behaviour of beams retrofitted by CFRP. Two models were used to represent the interface between CFRP and concrete, a perfect bond model and a cohesive model. Validation of the model was performed using data obtained from an experimental study. The results showed that the cohesive model is able to simulate the composite behaviour of reinforced concrete beams retrofitted by CFRP in shear correctly. The model is then used to examine the influence of length and orientation of CFRP. It is shown that the length of CFRP and the orientation strongly influence on the behaviour of the retrofitted beams.

1 INTRODUCTION

Reinforced concrete (RC) structural elements such as beams are subjected to significant flexure and shear. Strengthening or upgrading becomes necessary when these structural elements are not able to provide satisfactory strength and serviceability. Shear failure of RC beams could occur without any warning. Many existing RC members are found to be deficient in shear strength and need to be repaired. Shear deficiencies in reinforced concrete beams may occur due to many factors such as inadequate shear reinforcement, reduction in steel area due to corrosion, use of outdated design codes, increased service load and design faults.

The application of carbon fibre reinforced polymer (CFRP) as an external reinforcement has become widely used recently. It is found to be important for improving the structural performance of reinforced concrete structures. A beam can be bonded with CFRP plates on either the soffit or the web. Generally, the soffit bonding is preferred for flexural retrofitting of beams, while web bonding is performed for shear retrofitting. For shear retrofitting of beams, different schemes can be employed, such as bonding vertical or inclined strips, or bonding continuous plates on the web. Most of the research done in the past on strengthening of existing RC beams focused on flexural strengthening (Ashour et al. 2004), (Esfahani et al. 2007), (Wang & Zhang 2008) (Wenwei & Guo 2006) and (Obaidat et al. 2009) and very few studies have specifically addressed the topic of shear strengthening (Sales & Melo 2001), (Santhakumar & Chandrasekaran 2004) and (Sundarraja & Rajamohan 2009).

While experimental methods of investigation are extremely useful in obtaining information about the composite behaviour of FRP and reinforced concrete, the use of numerical models helps in developing a good understanding of the behaviour at lower costs.

In this paper, the efficiency of applying CFRP as external reinforcement to enhance the shear capacity of RC beams was investigated by the finite element method. ABAQUS (Hibbitt, Karlsson, & Sorensen Inc. 2000) is used to model the behaviour of a retrofitted beam; in the first part of the paper validation of the model is done using four beams tested by Obaidat (Obaidat 2007). The second part is to investigate the effect of different parameters on shear retrofitting. The test parameters included a variable length and orientation of CFRP.

2 EXPERIMENTAL DATA

The experimental data was obtained from (Obaidat 2007). This work consisted of four beams subjected to four point bending. All beams were identical in geometry and reinforcement. The geometry of the beams is shown in Figure 1 and the material properties are given in Table 1. Two beams were used as control beams and the rest were retrofitted on both sides of the beams with CFRP. The CFRP had 50 mm width and 300 mm length and the spacing was 100 mm, see Figures 2 and 3.

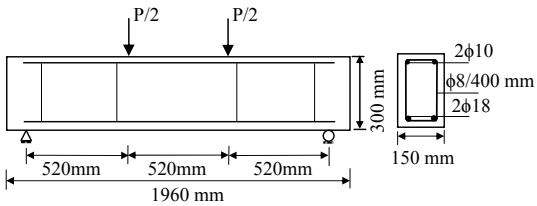

Figure 1. Geometry, arrangement of reinforcement and load of the tested beams.

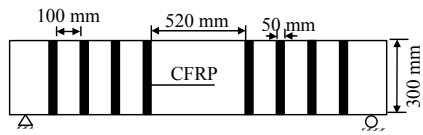

Figure 2. The arrangement of the CFRP laminate in retrofitted beams.

Figure 3. Installation CFRP in experimental work.

Table.1. Mechanical properties of materials used.

Steel	f_y	507 MPa
	E_s	210 GPa
	ν	0.3
Concrete	f_c'	30 MPa
CFRP	E_f	165 GPa
	f_f	2 GPa

3 NUMERICAL SIMULATIONS

3.1 *Studied bodies*

In order to study how the length and orientation of CFRP affect the shear behaviour of retrofitted beams, numerical simulations were conducted for the cases shown in Figure 4. Three different lengths of CFRP were used in the simulations. The orientation of the CFRP was also varied keeping the amount of CFRP as in 90º by using 35 mm width of CFRP. Two different models for the concrete-CFRP interface were evaluated in the validation.

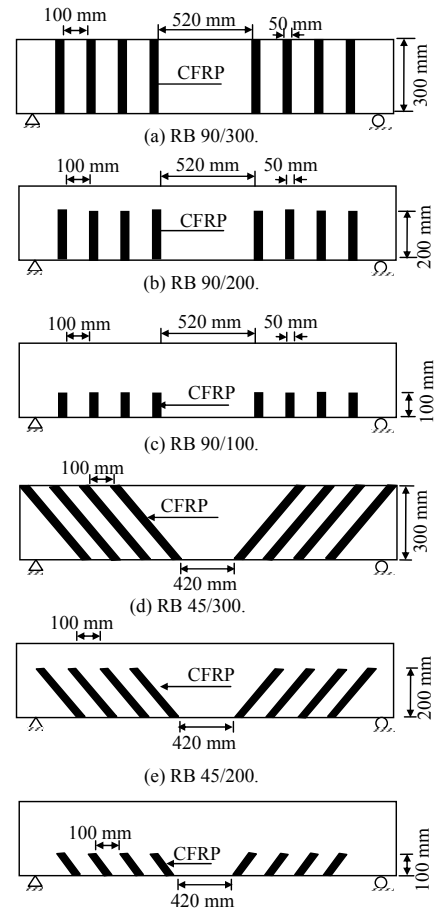

Figure 4. Studied CFRP configurations.

3.2 *Material Models*

3.2.1 *Concrete*

A plastic damage model was used to represent the behaviour of concrete. The model assumes that the two main failure mechanisms are tensile cracking and compressive crushing of the concrete material.

The softening curve of concrete under tension is shown in Figure 5, where f_{ct} is the tensile strength, and G_f is the fracture energy of concrete, (Hillerborg 1985). The tensile strength of concrete can be obtained from Equation 1 (ACI Comitte 318. 1999), and the fracture energy was assumed equal to 90 J/m^2.

$$f_{ct} = 0.35\sqrt{f_c'} = 1.81 \text{ MPa} \quad (1)$$

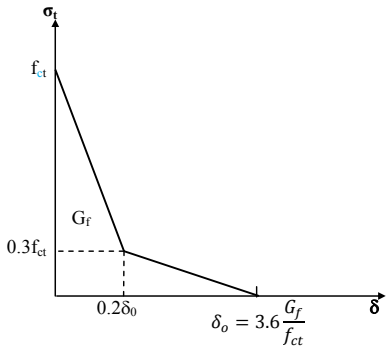

Figure 5. Softening curve of concrete under uni-axial tension.

The stress-strain curve under uni-axial compression is shown in Figure 6, (Saenz 1964). The modulus of elasticity was obtained using (ACI Comitte 318. 1999)

$$E_c = 4700\sqrt{f_c'} = 26000 \text{ MPa} \quad (2)$$

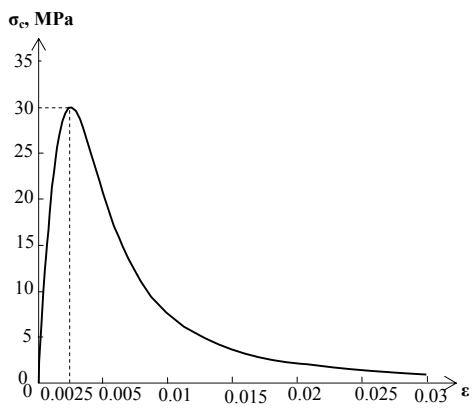

Figure 6. Stress-strain behaviour of concrete under uniaxial compression.

3.2.2 *Steel reinforcement*

The constitutive behaviour of steel was modelled using an elastic perfectly plastic model, see Figure 7. The parameters used to define this model are elastic modulus E_s, yield stress, f_y, and Poisson's ratio, ν. The parameters from the experimental study were used; see Table 1. Perfect bond was assumed between the steel and the concrete.

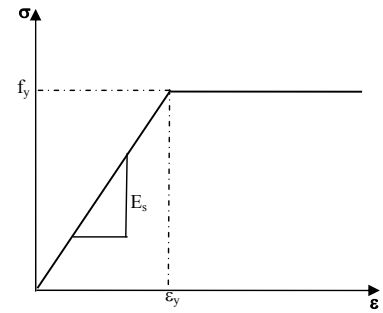

Figure 7. Stress-strain curve for the reinforcement steel.

3.2.3 *CFRP*

The CFRP was assumed to be a linear elastic orthotropic material. The elastic modulus in the fibre direction of the unidirectional CFRP material used in the experimental study was specified by the manufacturer as 165 GPa. For the orthotropic material model E_{11} was set to 165 GPa. Using Rule of Mixture (Piggott 2002), E_{epoxy}= 2.5 GPa and the fibre volume fraction 75 %, E_{fibre} was found to be 219 GPa and ν_{12}= ν_{13}= 0.3. By use of Inverse Rule of Mixture (Piggott 2002), E_{22}= E_{33}= 9.65 GPa and G_{12}=G_{13}= 5.2 GPa. ν_{23} and G_{23} were set to 0.45 and 3.4 GPa, respectively.

3.2.4 *CFRP-concrete interface*

Two different models for the interface between CFRP and concrete were used in this study. In the first model, the interface was considered as a perfect bond. In the second model, the interface was modelled using a cohesive zone model.

Cohesive elements were used together with a traction separation law which defines the traction as a function of the separation distance between the interface elements, see Figure 8. The material has an initial linear elastic behaviour. The elastic response is followed by damage initiation and evolution until total degradation of the elements.

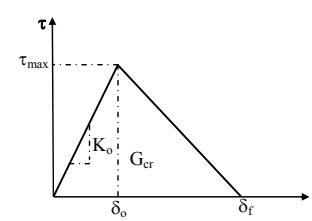

Figure 8. Bilinear traction–separation constitutive law.

The nominal traction stress vector consists of three components: σ_n, τ_t, τ_s, which represents the normal and shear tractions, respectively.

The initial stiffness matrix is directly related to the thickness of the cohesive layer and to the material stiffness G. A general expression of this relation is:

$$K_o = \frac{1}{\frac{t_i}{G_i}+\frac{t_c}{G_c}} \quad (3)$$

where t_i is the adhesive thickness, t_c is the concrete thickness, and G_i and G_c are the shear modulus of adhesive and concrete respectively.

An upper limit for the maximum shear stress, τ_{max}, is provided by the expression (Ye, Lu & Chen 2005):

$$\tau_{max} = 1.2\,\beta_w f_{ct} \quad (4)$$

where:

$$\beta_w = \sqrt{\left(2.25 - {}^{w_f}/_{s_f}\right)/\left(1.25 + {}^{w_f}/_{s_f}\right)}$$

and w_f is CFRP plate width, s_f is spacing of CFRP strips and f_{ct} is concrete tensile strength.

This equation gives τ_{max}= 2.17 MPa. Numerical simulations showed that this value is too high; since CFRP rupture or concrete crushing induced the failure, instead of the CFRP debonding that occurred in the experimental study. Hence, τ_{max} was reduced to 1.5 MPa.

For fracture energy, G_{cr}, previous studies have indicated values from 300 J/m^2 up to 1500 J/m^2 (JCI 1998) and (JCI 2003). For this study the value 900 J/m^2, in the middle of the interval proposed by previous studies, was used.

During separation of the cohesive element surfaces, the thickness increases and the stiffness degrades. The quadratic nominal stress criterion was used as damage initiation criterion:

$$\left\{\frac{\langle\sigma_n\rangle}{\sigma_n^o}\right\}^2 + \left\{\frac{\langle\tau_s\rangle}{\tau_s^o}\right\}^2 + \left\{\frac{\langle\tau_t\rangle}{\tau_t^o}\right\}^2 = 1 \quad (5)$$

where σ_n and τ_s, τ_t are the cohesive tensile and shear strengths of the interface. The values used for this study were σ_n^o= f_{ct}= 1.81 MPa, and τ_s^o= τ_t^o=1.5 MPa.

3.3 *Finite Element Analysis*

The concrete and the steel were modelled using a linear tetrahedral element. This element has four nodes with three degrees of freedom at each node– translation in the x, y, and z directions. The element used is capable of plastic deformation and cracking in three orthogonal directions. An eight node reduced-integration element was used to model the CFRP composite and the steel plates under the load and at the support. This element also has three degrees of freedom at each node. Eight-node 3-D cohesive elements were used to model the interface layer. The cohesive interface elements are composed of two surfaces separated by a thickness. The relative motion of the bottom and top parts of the cohesive element measured along the thickness direction represents opening or closing of the interface. The relative motion of these parts represents the transverse shear behaviour of the cohesive element.

Abaqus/standard (Hibbitt, Karlsson, & Sorensen Inc. 2000) was used for these simulations. The total deflection applied was divided into a series of deflection increments. In addition automatic stabilization and small time increments were used to avoid a diverged solution. Since the geometry of the beams, loading and boundary conditions were symmetrical, only one quarter of a beam was modelled with typical finite element mesh as shown in Figure 9. Boundary conditions are shown in Figure 10.

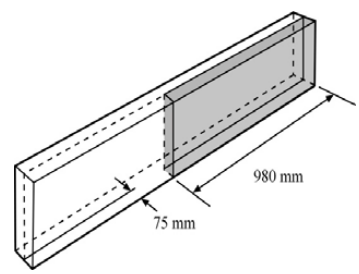

(a) By use of symmetry, one quarter of the beam was modelled.

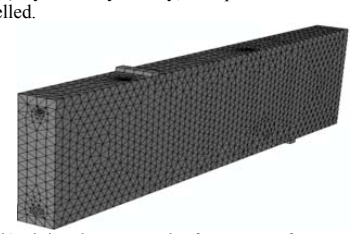

(b) Finite element mesh of a quarter of a control beam.

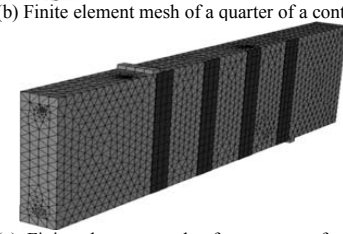

(c) Finite element mesh of a quarter of a strengthened beam.

Figure 9. Geometry and elements used in the numerical analysis.

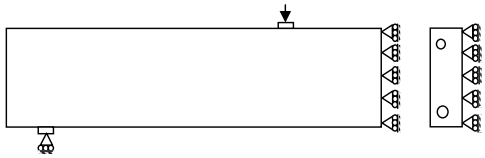

Figure 10. Boundary conditions used in numerical work.

4 VERIFICATION OF FINITE ELEMENT MODEL

To verify the finite element model of the reinforced concrete retrofitted with CFRP, four beams from an experimental study (Obaidat 2007) were simulated. The results from the FEM analysis were then compared with the experimental results.

The load-deflection curves for the control beams are shown in Figure 11. In the linear part the FEM results are slightly stiffer than the experimental results. One explanation for this may be the assumption of perfect bond between concrete and steel.

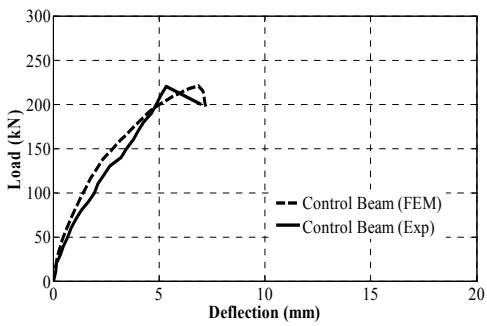

Figure 11. Load-deflection curves of control beams obtained by experiments and FEM.

As shown in Figure 12 there is good agreement between the cohesive model and the perfect bond model in the first part of the curve, but when the crack starts to propagate the cohesive bond model gives a stronger softening effect in the beam. It is also clear from the figure that the cohesive model shows a very satisfactory agreement with the experimental response. The perfect bond model overestimates the ultimate load and deflection. This can be attributed to the fact that the perfect bond model fails to capture the softening of the beam and it is not able to represent the debonding failure that occurred in the experimental work.

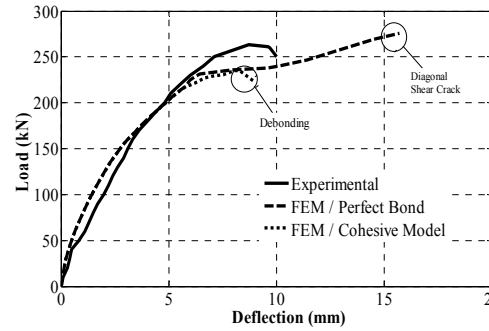

Figure 12. Load-deflection curves of retrofitted beams obtained by experiments and FEM.

The cohesive model also shows good agreement with the experimental work in the debonding failure mode as shown in Figure 13. The following results have been obtained using the cohesive model.

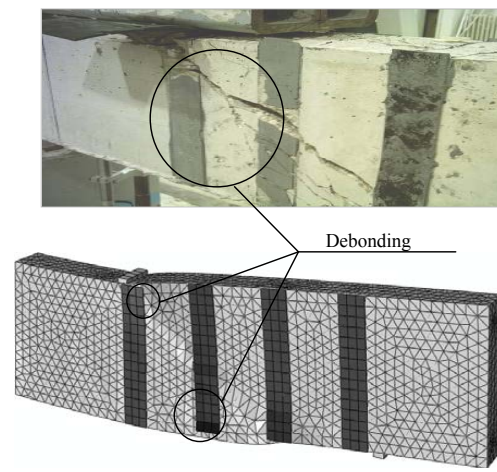

Figure 13. Comparison of failure mode from FEM analysis and experiment.

5 RESULTS AND DISCUSSION

5.1 *Effect of length of CFRP*

To study the effect of CFRP length, three lengths were investigated, 100 mm (lower third of web of beam, RB 90/100), 200 mm (lower two thirds of web of beam, RB 90/200) and 300 mm (entire web of beam, RB 90/300).

Figure 14 shows the load versus the mid-span deflection of a reinforced concrete beam retrofitted with CFRP. In all beams the failure mode was debonding due to concentration of shear stress resulting from the diagonal crack.

Generally the stiffness and load capacity of the beam increases when the length of CFRP is equal to the web of the beam as shown in Figure 14.

In Figure 14, it can be seen that for RB 90/200 and RB 90/100 the reinforcement seems not to strengthen the beam; this is due to the fact that the crack crossed the strips close to their end. This result supports what (Monti and Liotta 2005) found. For these cases the formation of such a crack was accompanied by yielding of internal shear reinforcement. The steel yielding caused the drop in the beam stiffness compared to the control beam as shown in Figure 14. Before the yielding any increase in loading is shared by the reinforcing steel and CFRP. After the yielding most of the increased loading has to be carried by the plate until debonding occurs.

It can be seen also that RB 90/200 failed at a lower load than RB 90/100. This is attributed to the fact that the area in the middle of the web is critical in the failure process and that the end of plate in RB 90/200 is in that area. Hence the stress concentration is more pronounced in this beam and debonding occurs earlier.

This analysis, regarding the length of CFRP, verifies that the strip, when the orientation is 90 degrees, should cover the whole web of the beam to provide an improvement of beam behaviour.

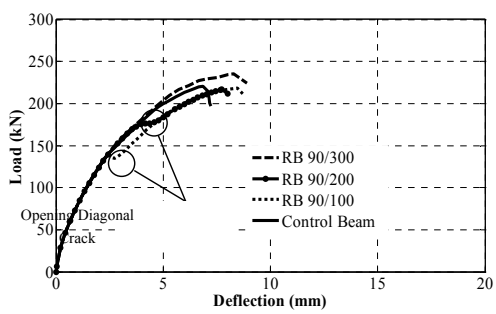

Figure 14. Load-deflection curves for different lengths of CFRP, obtained by FEM.

5.2 *Effect of orientation of CFRP*

Since a shear crack propagates in a diagonal manner the orientation of the CFRP may affect the behaviour of a retrofitted beam. Two orientations, 90º and 45º were studied.

For the longest CFRP the failure mode was a shear crack while for the other beams the failure mode was debonding.

It is clear from Figure 15 that when the angle of orientation was 45º the retrofitted beam carries more load for all lengths.

It is interesting to note that the load capacity for RB 45/300, RB 45/200 and RB 45/100 was increased by 20.1 %, 2% and 5% respectively, compared to the control beam while the change was 11.9% for RB 90/300, -1.8% for RB 45/200 and -1.1% for RB 90/100. This indicates that the performance of a beam retrofitted with CFRP is influenced by the orientation of the CFRP. When the CFRP did not cover the full depth of the beam the load capacity was actually decreased for 90º, while a small increase was obtained for 45º.

From Figure 16, it can be concluded that the orientation of CFRP has a strong effect on the behaviour of the retrofitted beam for the same total amount of CFRP. A 45º orientation gives a better effect in terms of maximum load and deflection.

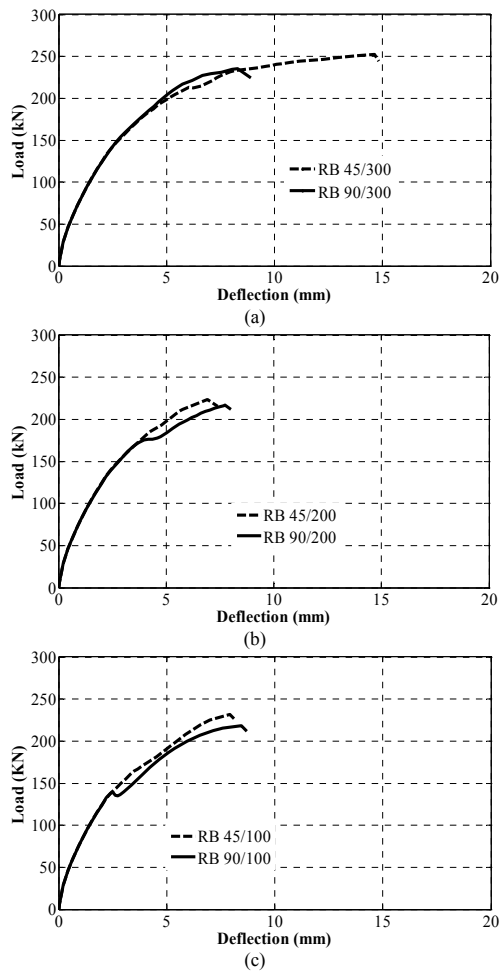

Figure 15. Load-deflection curves of 90º and 45º of CFRP obtained by FEM.

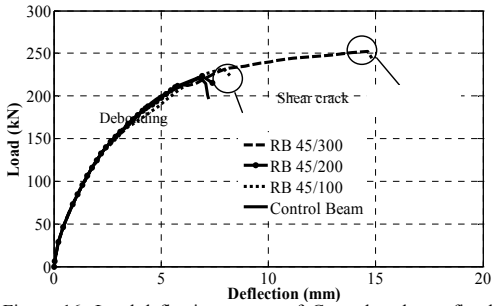

Figure 16. Load-deflection curves of Control and retrofitted beams with 45° of CFRP and different lengths, obtained FEM.

6 CONCLUSION

An FE model was used to investigate the behaviour of RC beams retrofitted in shear with CFRP by using the commercial program ABAQUS. The results from FE model were compared with experimental work by Obaidat (Obaidat 2007) to assess the accuracy of the proposed FEM model. The present numerical study has shown that the proposed FEM model is suitable for predicting the behaviour of RC beams retrofitted with CFRP plates in shear. It should also be noted that the perfect bond model cannot account for debonding failure of CFRP since this model does not take in to account the behaviour of the interface between the CFRP and the concrete. On the other hand, the cohesive model is capable to predict the debonding failure. This study also presents results of an investigation of the effects of length and orientation of CFRP. The following can be concluded:

(1) Change in length of CFRP reinforcement may result in different behaviours of retrofitted beams. The longest CFRP presents a high stiffness and high load while when the CFRP strip do not cover the full depth of beam the load capacity decrease for 90º. Therefore it is not advisable to use a CFRP strip not covering the entire beam depth when retrofitting for shear.

(2) The peak load and deflection is slightly affected by the orientation of CFRP. For 45º CFRP orientation, a larger increase in load capacity is obtained compared to 90 º.

7 REFERENCES

ACI Comitte 318. 1999. Building Code Requirements for Structural Concrete and Commentary (ACI 318-99). American Concrete Institute Detroit, MI.

Ashour, AF, El-Refaie, SA & Garrity, SW. 2004. Flexural strengthening of RC continuous beams using CFRP laminates. *Cement & Concrete Composites;* 26: 765- 775.

Esfahani, M., Kianoush, M., & Tajari. 2007. A. Flexural behaviour of reinforced concrete beams strengthened by CFRP sheets. *Engineering Structures*; 29: 2428-2444.

Hibbitt, Karlsson, & Sorensen, Inc. 2000. ABAQUS Theory manual, User manual Example Manual, Version 6.7. Providence, RI.

Hillerborg, A. (1985). The theoretical basis of a method to determine the fracture energy G_F of concrete. Materials and Structures, RILEM 50-FMC, 108, pp 291-296.

JCI. Technical report on continous fibre reinforced concrete. JCI TC952 on Continous Reinforced Concrete 1998; 116-124.

JCI. Technical report on retrofit technology for concrete structures. Technical Committee on Retrofitting Technology for Concrete Structures 2003; 79-97.

Monti, G., & Liotta, M. A. 2005. FRP strengthening in shear: Test and design equations. *Proceeding of 7th International Symposium on Fiber Reinforce Polymer for Reinforced Concrete Structures (FRPRCS-7)*; 543-562.

Obaidat,Y. 2007. Retrofitting of reinforced concrete beams using composite laminates, *Master Thesis, Jordan University of Science and Technology.*

Obaidat,Y.,Heyden,S., & Dahlblom, O. 2009.The Effect of CFRP and CFRP/ Concrete Interface Models when Modelling Retrofitted RC Beams with FEM. Accepted for publication in *Composite Structures*.

Piggott, M. Load bearing fibre composites, 2nd Edition. Kluwer Academic Publishers, Boston/ Dordrecht/ London, 2002.

Saenz, L. Equation for the stress-strain curve of concrete. Desayi P, Krishnan S. ACI Journal 1964; 61:1229–35.

Salles Neto, M., Melo, G.S., Nagato, Y., T Beams Strengthened in shear with carbon sheet laminates, Fiber-reinforced Plastic for Reinforced Concrete Structure 2001; 1: 239-248.

Santhakumar, R., & Chandrasekaran, E. 2004. Analysis of retrofitted reinforced concrete shear beams using carbon fibre composite. Electronic *Journal of Structural Engineering,* 4: 66-74.

Sundarraja, M., & Rajamohan, S. 2009. Strengthening of RC beams in shear using GFRP inclined strips – An experimental study. *Construction and building materials,* 23: 856-864.

Wang, J., & Zhang, C. 2008. Nonlinear fracture mechanics of flexural- shear crack induced debonding of FRP strengthened concrete beams. I*nternational journal of solid and structures,* 45: 2916-2936.

Wenwei W., Guo L. 2006. Experimental study and analysis of RC beams strengthened with CFRP

laminates under sustaining load. *International Journal of Solids and Structures* 2006; 43: 1372–1387.

Ye, L. P., Lu, X. Z, and Chen, J. F. Design proposals for the debonding strengths of FRP strengthened RC beams in the chinese design code. *Proceeding of International Symposium on Bond Behaviour of FRP in Structures* (BBFS 2005); 45-54.

Paper D

D

FEM Study on the Effect of CFRP Stiffness and Width on Retrofitted Reinforced Concrete Beam Behaviour

Yasmeen Taleb Obaidat, Susanne Heyden and Ola Dahlblom

Submitted to Composite Structures

FEM Study on the Effect of CFRP Stiffness and Width on Retrofitted Reinforced Concrete Beam Behaviour

Yasmeen Taleb Obaidat*, Susanne Heyden and Ola Dahlblom

Division of Structural Mechanics, Lund University, Lund, Sweden

Abstract

The finite element program ABAQUS was used to study the effect of different parameters on the behaviour of an RC beam retrofitted with carbon fibre reinforced polymer (CFRP). These parameters were the stiffness and width of the CFRP. A linear elastic isotropic model was used for the CFRP and a cohesive bond model was used for the concrete–CFRP interface. A plastic damage model was used for the concrete. The material models were validated against experimental work and the results showed good agreement between experimental data and numerical results. Observations indicate that the CFRP width to beam width ratio and CFRP stiffness influence the type of failure mode of a beam retrofitted with CFRP. For small width and for large value of stiffness debonding will occur before steel yielding due to stress concentration at the end of the plate. For small values of stiffness, rupture of CFRP will occur. It was found that when the stiffness of CFRP increases the maximum load increases until a certain value of stiffness, then the maximum load decreases again. Simulations also show that the external load at steel yielding and the maximum load increase with the CFRP width.

Keywords: Carbon fibre reinforced polymer (CFRP), FEM (finite element method), Retrofitting, Reinforced concrete beam, Debonding.

1. Introduction

Upgrading of reinforced concrete structures may be required for many different reasons. The concrete may have become structurally inadequate, for example due to deterioration of materials, poor initial design and/or construction, lack of maintenance, upgrading of design loads or accident events such as earthquakes.

Retrofitting of concrete structures with externally bonded reinforcement is generally done by using either steel plates or fibre reinforced polymer (FRP) laminates. FRP can be convenient compared to steel for a number of reasons. They are lighter than the equivalent

* Corresponding author.
E-mail address: Yasmeen.Obaidat@construction.lth.se

steel plates. They can be formed on site into complicated shapes and they can also be easily cut to length on site. The installation is easier and temporary support until the adhesive gains its strength is not required due to the light weight of FRP. Earlier research has demonstrated that the addition of FRP laminate to reinforced concrete beams can increase stiffness and maximum load and reduce crack widths [1], [2], [3] and [4] and the technique is often used for upgrading concrete structures.

Nonlinear finite element analysis can be used to study the behaviour of retrofitted structures. This reduces the time and cost needed for experimental work. Many researchers have simulated the behaviour of retrofitted reinforced structures by using the finite element method. Several different approaches have been considered. Some models use nonlinear elasticity or plasticity models to capture the more complicated effects and predict the behaviour of reinforced concrete retrofitted by FRP in a general sense, [5], [6], [7], [8] and [9]. An important issue is the influence of the properties of the interface between the carbon fibre reinforced polymer (CFRP) and the concrete. This was modelled in [10]. In this paper the model developed in [10] was used for a parametric study.

The lack of design standards is disadvantageous to external strengthening of structures with CFRP. Developing rational design guidelines requires a fundamental understanding of the performance of structures strengthened with CFRP. The aim of this paper is to contribute to the understanding of the influence of CFRP width and stiffness on the performance of a strengthened beam.

2. Full Scale Experiment

Reinforced beams that were previously tested, Obaidat [11], were used to validate the FE procedure discussed in the following sections. Fig. 1 shows the tested beams. A summary of the properties of materials as reported by Obaidat [11] is shown in Table. 1. Two control beams were loaded to failure. Two other beams were loaded until cracks appeared, then retrofitted with unidirectional CFRP laminates attached to the bottom and finally loaded to failure. The fibres were oriented along the length of the beam. The laminates were 1560 mm long, 50 mm wide and 1.2 mm thick.

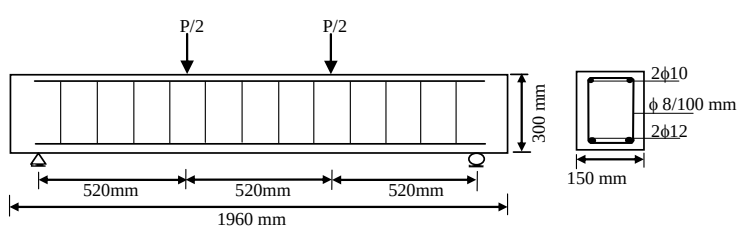

Fig. 1. Geometry, arrangement of reinforcement and load of the tested beams.

Table. 1. Mechanical properties of materials used.

		Obaidat [11]	
Steel	f_y	507	MPa
	E_s	210	GPa
	ν	0.3	
Concrete	f_c'	30	MPa
CFRP	E_{CFRP}	165	GPa
	f_{CFRP}	2	GPa

3. Finite Element Model

Beams with the same geometry, reinforcement and loading as in the experimental study, Fig. 1, were modelled by means of the finite element method. To account for the cracks that were present at retrofitting, a pre-crack was introduced close to midspan.

The analysis was performed using the general purpose finite element computer program ABAQUS [12]. By taking advantage of the symmetry of the beams, a quarter of the full beam was used for modelling, see Fig. 2. This approach reduced computational time and computer disk space requirements significantly.

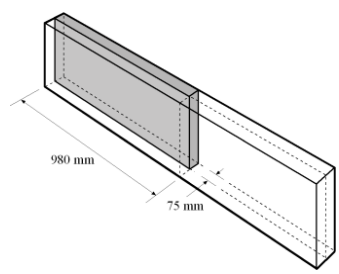

(a) A quarter of the beam was modelled.

(b) Finite element mesh of quarter of beam.

Fig. 2. Geomtry and mesh used in the numerical analysis.

The reinforced concrete and steel loading plate were modelled using linear tetrahedral elements. The pre-crack was modelled by making a gap of 0.1 mm width and 10 mm depth between the continuum elements, 20 mm from the centre of beam.

4. Material Properties

4.1. Concrete:

The damage plasticity concrete model in ABAQUS/Standard [12] assumes that the main two failure mechanisms are tensile cracking and compressive crushing. The evolution of the yield (or failure) surface is linked to failure mechanisms under tension and compression loading.

Under uniaxial tension the stress-strain response follows a linear elastic relationship until the value of the failure stress, f_{ct} is reached. The failure stress corresponds to the onset of micro-cracking in the concrete material. Beyond the failure stress the formation of micro-cracks is represented macroscopically with a softening stress-strain response. Hence, the parameters required to establish the first part of the relation are elastic modulus, E_c, and tensile strength, f_{ct}. From the compressive strength which is reported in [11], the elastic modulus and concrete tensile strength are calculated according to [13].

$$f_{ct} = 0.35\sqrt{f_c'} \tag{1}$$

$$E_c = 4700\sqrt{f_c'} \tag{2}$$

where f_c', f_{ct} and E_c are given in MPa.

The parameter associated with the softening part of the curve is fracture energy, G_f. The fracture energy for mode I, G_f, is the area under the softening curve and is according to [14] estimated as

$$G_f = G_{fo}\left(\frac{f_c'}{10}\right)^{0.7} \tag{3}$$

where G_{fo} is a constant value related to maximum aggregate size and f_c' is given in MPa The crack opening is calculated from the fracture energy; see Fig. 3 [15].

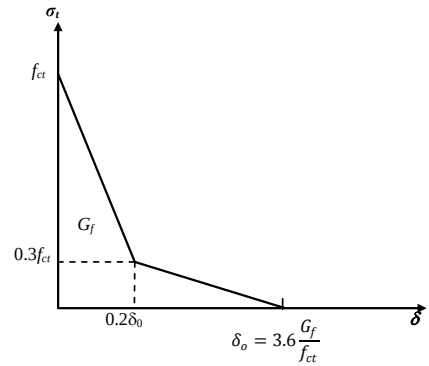

Fig. 3. Softening curve of concrete under uni-axial tension.

Under uniaxial compression the response is linear until the value of initial yield, f_{co}. In the plastic regime the response is typically characterized by stress hardening followed by strain softening beyond the ultimate stress, $f_c^{'}$. The stress–strain relationship proposed by Saenz [16] was used to describe the uniaxial compressive stress–strain curve for concrete:

$$\sigma_c = \frac{E_c \varepsilon_c}{1 + (R + R_E - 2)\left(\frac{\varepsilon_c}{\varepsilon_o}\right) - (2R - 1)\left(\frac{\varepsilon_c}{\varepsilon_o}\right)^2 + R\left(\frac{\varepsilon_c}{\varepsilon_o}\right)^3} \tag{4}$$

where:

$R = \frac{R_E(R_\sigma - 1)}{(R_\varepsilon - 1)^2} - \frac{1}{R_\varepsilon}, \quad R_E = \frac{E_c}{E_o}, \quad E_o = \frac{f_c^{'}}{\varepsilon_o}$

and,

$R_\varepsilon = 4$, $R_\sigma = 4$ as reported in [17], and ε_o=0.0025.

4.2 Steel reinforcement and steel plate:

The steel was assumed to be elastic-perfectly plastic and identical in compression and tension. Perfect bond was assumed between the steel and concrete.

4.3 CFRP composite:

The CFRP was modelled as an isotropic linear elastic material throughout this study. The unidirectional CFRP composite actually shows an orthotropic behaviour, but it was shown in [10] that only the axial modulus is of importance in an application of this type. The elastic modulus and strength were taken to be E_{CFRP}=165 GPa and f_{CFRP}=2 GPa respectively, as

found in the experimental study. The Poisson ratio of the CFRP composite was assumed to be ν_{CFRP}=0.30.

4.4. Interface Layer

Since Obaidat [10] found that a cohesive model is able to describe the failure mode and load capacity accurately, this was used to represent the interface between the concrete and CFRP in this study.

Cohesive elements were used together with a traction separation law which defines the traction function of the separation distance between interface elements [18], Fig. 4. The material has an initial linear elastic behaviour. The elastic response is followed by damage initiation and evolution until total degradation of the elements.

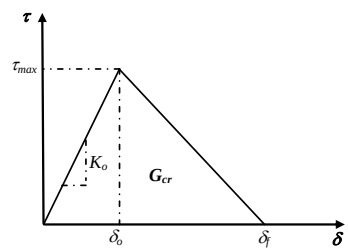

Fig. 4. Bilinear traction – separation constitutive law.

The behaviour of the interface prior to initiation of damage is described as linear-elastic. The nominal traction vector consists of three components in three-dimensional problems: σ_n, τ_t, τ_s, which represent the normal and shear tractions, respectively.

The stiffness is determined according to

$$K_o = \frac{1}{t_i/G_i + t_c/G_c} \tag{5}$$

where t_i is the adhesive thickness, t_c is the effective thickness of concrete whose deformation forms part of the interfacial slip and was taken as 5 mm, and G_i= 0.667 GPa and G_c=10.8 GPa are the shear modulus of adhesive and concrete respectively.

The quadratic nominal stress criterion was used as damage initiation criterion

$$\left\{\frac{\sigma_n}{\sigma_n^o}\right\}^2 + \left\{\frac{\tau_s}{\tau_s^o}\right\}^2 + \left\{\frac{\tau_t}{\tau_t^o}\right\}^2 = 1 \tag{6}$$

where σ_n, τ_s and τ_t are the cohesive tensile and shear stresses of the interface, and the subscript refers to the direction of the stress component. The values used for this study were

$\sigma_n^o = f_{ct}$= 1.81 MPa and $\tau_s^o = \tau_t^o = \tau_{max}$. An upper limit for the maximum shear stress, τ_{max}, is provided by the expression [19]

$$\tau_{max} = 1.5\,\beta_w f_{ct} \tag{7}$$

where

$$\beta_w = \sqrt{(2.25 - w_{CFRP}/w_{beam})/(1.25 + w_{CFRP}/w_{beam})}$$

and w_{CFRP} is CFRP plate width, w_{beam} is beam width and f_{ct} is concrete tensile strength. This equation gives τ_{max}= 3 MPa for w_{CFRP}= 50 mm. In numerical simulations using this value, failure is initiated by CFRP rupture or concrete crushing, instead of the CFRP debonding that occurred in the experimental study, indicating that this value is too high; hence, τ_{max} was reduced to 1.5 MPa.

For fracture energy, G_{cr}, previous studies have indicated values from 300 J/m^2 up to 1500 J/m^2 [20] and [21]. For this study the value 900 J/m^2, in the middle of the interval proposed by previous studies, was used.

5. Validation of numerical model

The numerical model used for the parametric study was validated against the experimental results. Fig. 5a shows the load versus deflection curves at mid-span for the control beam. There is a good correlation between the experimental results and the numerical results. In Fig. 5b the load versus deflection curves at mid-span for the retrofitted beams are shown. It is clear that there is only a slight deviation between experimental data and numerical results. Hence, the proposed model proved to be able to simulate the composite behaviour of reinforced concrete beams retrofitted by CFRP successfully.

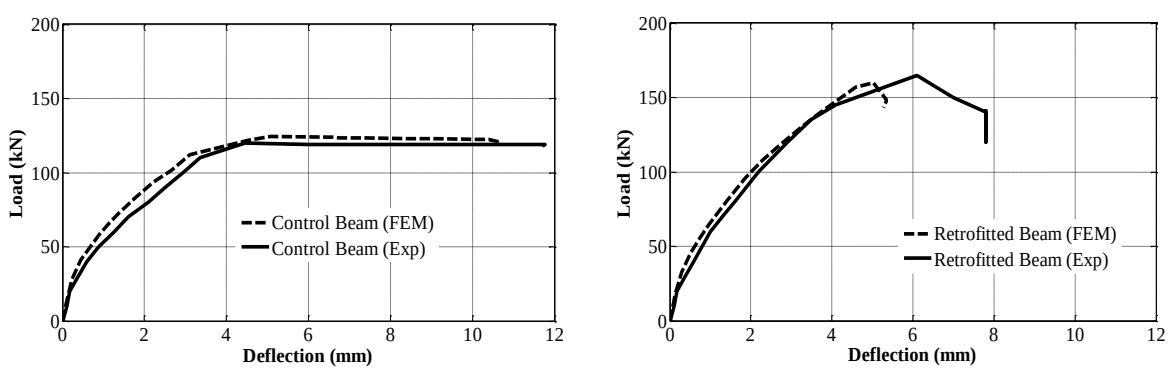

(a) Control Beam (b) Retrofitted Beam

Fig. 5. Comparison between load versus deflection curves from experimental and numerical studies.

6. Parametric Study

In order to study the effects of different parameters on a beam retrofitted with CFRP, numerical simulations were conducted. The most obvious parameter to vary is the total amount of external reinforcement, which is here quantified by the stiffness

$$K = E_{CFRP} \cdot w_{CFRP} \cdot t_{CFRP} \tag{8}$$

where E_{CFRP} is elastic modulus of CFRP, w_{CFRP} is CFRP width and t_{CFRP} is CFRP thickness. The value of the stiffness used in the experimental study is denoted K_o and has the numerical value

$$K_o = 165 \cdot 10^3 \,\mathrm{N/mm^2} \cdot 50\mathrm{mm} \cdot 1.2\,\mathrm{mm} = 9900\,\mathrm{N} \tag{9}$$

The series of different stiffnesses used to study the effect of varying stiffness, K, on retrofitted beams were: $0.25K_o$, $0.5K_o$, K_o, $2K_o$, $4K_o$ and $8K_o$. The values for the stiffness K used in the parametric study are shown on the vertical axis in Fig. 6.

Since there are three-dimensional effects present, the width of CFRP is also expected to be important. The width ratio, defined as

$$\mu = \frac{w_{CFRP}}{w_{beam}} \tag{10}$$

where w_{beam} is the beam width, was used as a measure for this. In the experimental study a width ratio of $\mu = \frac{50}{150} = \frac{1}{3}$ was used, and the values of μ used in the parameter study are shown on the horizontal axis in Fig. 6.

For varying the width ratio with constant stiffness, the thickness was chosen to adjust with the width, since simulation results show the same behaviour when adjusting either elastic modulus or thickness of CFRP to keep the stiffness, K, constant.

The dots in Fig. 6 indicate the points for which the load-deflection behaviour of the beam was simulated. For presenting the results, different groups were selected to study the effect of different parameters. In Group 1 the effect of varying width ratio with constant stiffness was examined. In Group 2 the effect of varying CFRP width was studied and Group 3 deals with the effect of varying thickness.

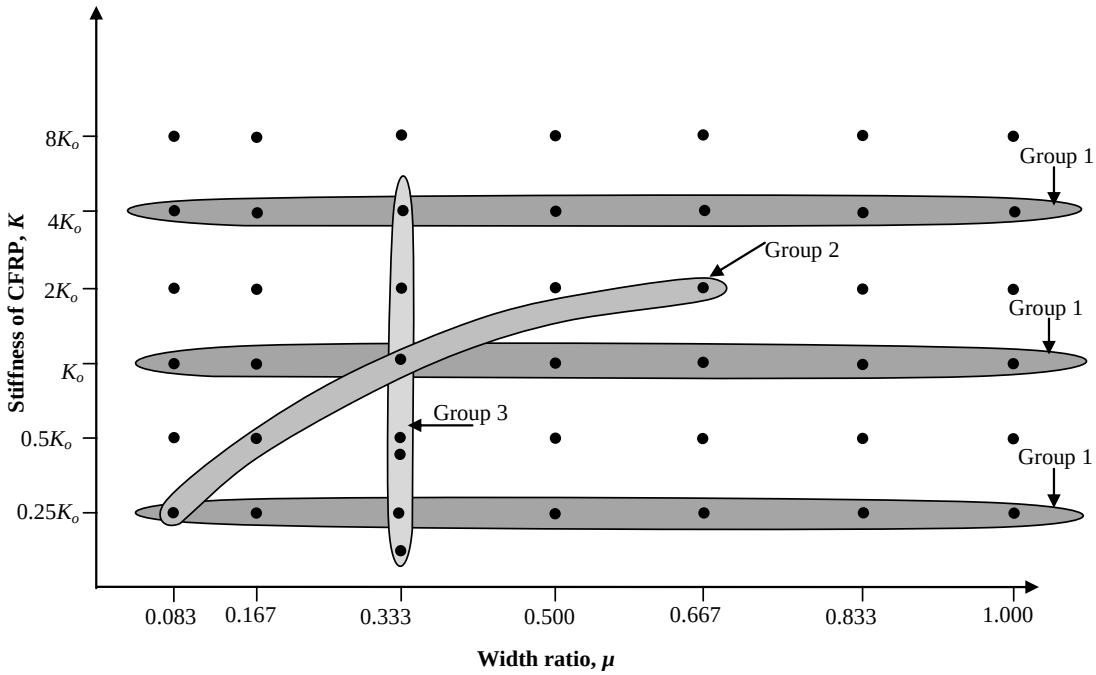

Fig. 6. Values for stiffness, K, and width ratio, μ, used in the parametric study. Dots indicate simulations.

7. Result and Discussion

As mentioned in section 6, the results were studied in three groups. Here the result of these groups will be discussed separately:

7.1. Group 1: Constant stiffness and varying width ratio

The main objective of this group is to obtain a clear understanding of how a certain amount of external reinforcement should be applied to get the best effect, and also under what circumstances more external reinforcement will give a better performance.

Several different failure modes were observed in this study. Fig. 7 illustrates under what circumstances the different failure modes occurred:

- *Debonding before steel yielding:*

This failure was observed for high value of the stiffness with any value of the width ratio and for small width ratio with any value of the stiffness. The plate end region could be regarded as an anchorage zone. In this zone axial force in the CFRP is built up through transfer of shear force in the CFRP-concrete bond. The stiffer the CFRP, the faster the increase in axial force, and hence the larger the shear stress in the bond. It is this stress concentration in the

plate end region that causes the debonding when the CFRP stiffness is high. The smaller the width ratio, the smaller is the bond area available to take part in the transfer of shear force. This is why this fracture mode tends to be limiting for small width ratios. As discussed in connection to Fig. 12, the stress transfer is somewhat higher for a higher width ratio, but this is a secondary effect.

- *Debonding at the plate end after steel yielding:*

This failure was observed for medium width ratios and medium stiffness. For these cases, where the CFRP stiffness is not so high and the width ratio is not so small, a larger build up of force is allowed in the CFRP before debonding occurs. This means that the bending moment can be increased to the extent that steel yielding occurs. At further load increase, however, debonding will occur in the plate end region.

- *Debonding at flexural crack after steel yielding:*

This failure was observed for high width ratios and medium stiffness. In this case, debonding due to stress concentration in the plate end region is not a limiting phenomenon. Also in this case the bending moment can be increased to the extent that steel yielding occurs. At further load increase, there is debonding but in this case it starts from maximum moment region and propagates towards the plate end. This is the result of high interfacial shear stresses at a flexural crack in the maximum moment region.

- *Debonding with concrete splitting:*

This failure was observed when using high width ratio with medium stiffness (lower stiffness than for the previous case). After steel yielding, a flexural shear crack will develop in the concrete. The crack will propagate to the level of the tensile reinforcement and extend horizontally along the bottom of the tension steel reinforcement. With increasing external load, the horizontal crack propagates to cause parts of the concrete cover to split with the CFRP plate.

- *CFRP rupture:*

This failure was observed for small stiffness with large width ratio. After steel yielding is initiated, the force carried by the steel cannot increase anymore. Hence further increase in bending moment will result in large force in the CFRP which leads to CFRP rupture in the mid-span region.

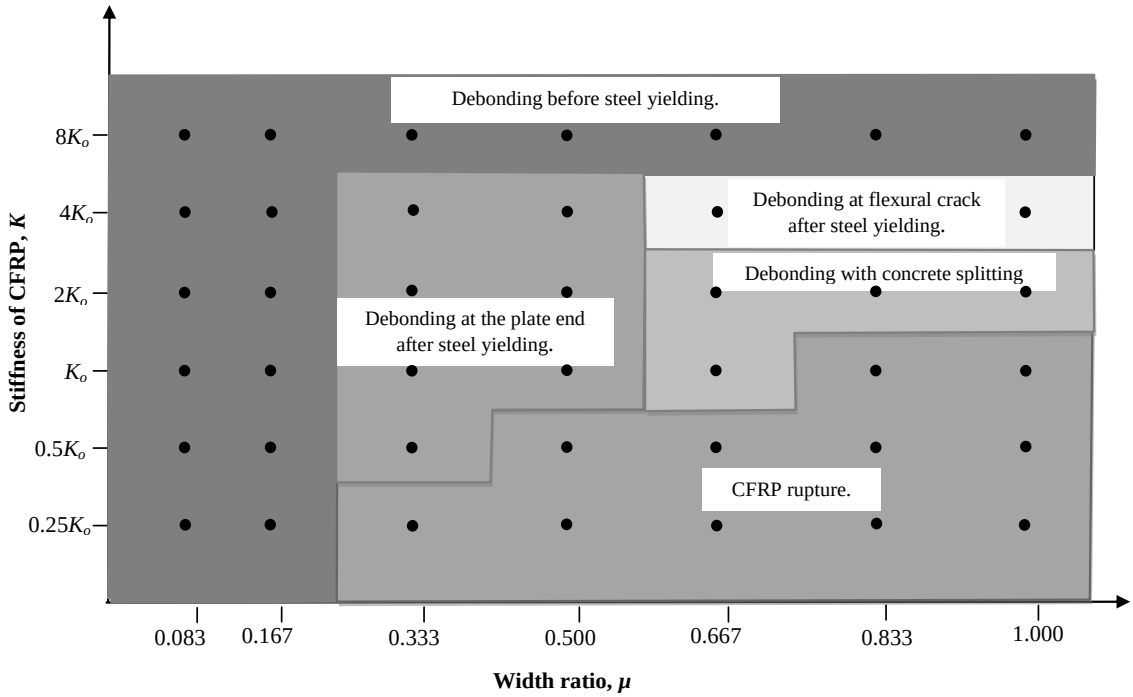

Fig. 7. Failure modes of the retrofitted beams. Data points are indicated with dots.

As is clear in Fig. 7, the width ratio and stiffness have a significant impact on the failure mode of the retrofitted beam.

The maximum load ratio is denoted α and defined as:

$$\alpha = \frac{\text{Maximum load, retrofitted beam}}{\text{Maximum load, control beam}}$$

Fig. 8a illustrates α as a function of the width ratio, μ, for stiffness values K=K_o, 0.5K_o and 0.25K_o, and Fig. 8b shows the corresponding values for stiffness values K=K_o, 2K_o, 4K_o and 8K_o.

For small stiffness values, Fig. 8a, the maximum load ratio, α, increases with the width ratio due to increase in the contact area between the concrete and CFRP. This allows the interfacial stress to distribute over a larger area, which means a less pronounced stress concentration and higher load before failure. When the failure mode shifts to CFRP rupture, which is for high width ratios, there is no further increase in the maximum load ratio. This is because at an increase in external load after steel yielding all additional axial load will be carried by the CFRP. A small CFRP stiffness means a small CFRP cross section area which in turn means a small ultimate load. This means that when CFRP rupture is the limiting phenomenon no positive effect is obtained from increasing the width ratio. For large width ratios the maximum load ratio increases with increased stiffness while the opposite occurs

when the width ratio has a low value. This can be attributed to the fact that when using small width with high value of stiffness a stress concentration occurs at the plate end and debonding occurs earlier. Fig. 8b shows maximum load ratio for high stiffness values. It is interesting to note that an increase in stiffness above K_o will actually give a decrease in maximum load ratio, at least if the width ratio is kept constant. For one data point this conclusion is, however, not valid. K= 2 K_o gives a higher value of α for μ= 1.

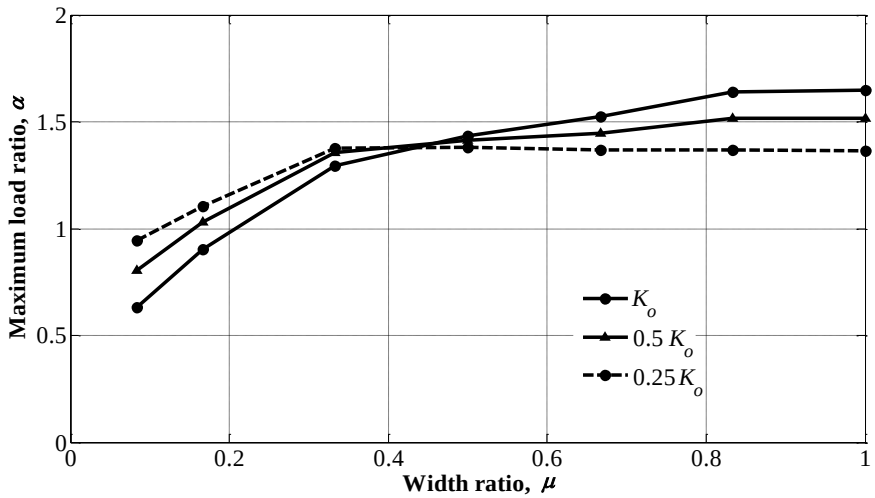

(a) Small stiffness values.

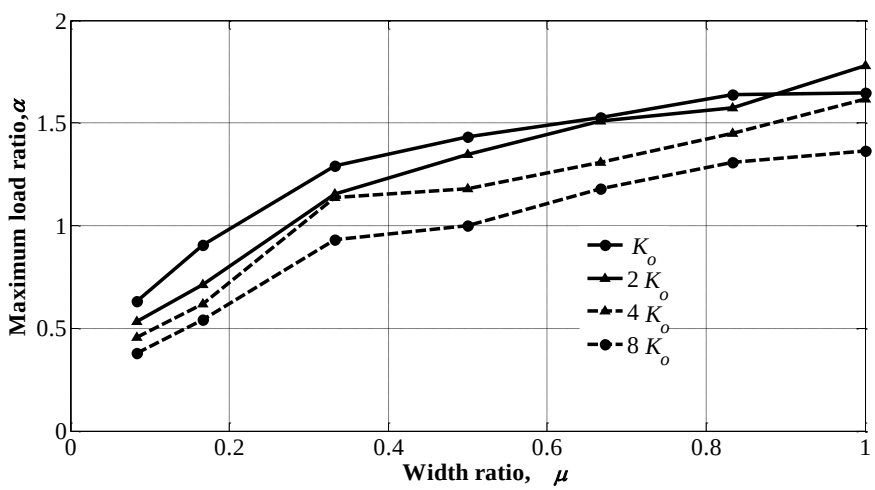

(b) Large stiffness values.

Fig. 8. Maximum load ratio, α, as a function of CFRP stiffness, K, and width ratio, μ.

In Fig. 9, Fig. 10 and Fig. 11, normalised load-deflection curves are shown for different width ratios for K=0.25K_o, K_o and 4K_o respectively. From the figures it can be observed that the load at steel yielding, maximum load and corresponding deflection increase with the width ratio.

A decrease in maximum load compared to the control beam was observed for small width ratio for all stiffness values. This is due to the fact that debonding occurs already at a small load. After debonding, these beams will probably behave like the control beam. Due to numerical instability at the debonding it is however not possible to follow the path towards the control beam curve.

It can be seen from Fig. 9, that when the stiffness, K, is small all beams have almost the same stiffness in the first part and it is close to the control beams. After cracks appear and steel yielding occurs in the control beam this looses in stiffness while the retrofitted beams can take a further load increase.

From Figs. 10 and 11 it can be seen, for the retrofitted beams, all curves are close to identical during the first part and slightly stiffer than the control beam. After the steel yielding and the debonding occur the curves drop and the deviation in stiffness appears.

In Figs. 9, 10, and 11 it can be seen that the width ratio affects the load at steel yielding. In order to clarify that a larger width ratio causes a larger part of the axial load to be carried by the CFRP, the axial stress in the centre of the CFRP along the beam is plotted in Fig. 12, at an external load level of 40 kN for K= 4K_o. From the plate end (right end of figure) the axial stress increases due to stress transfer from the concrete and due to increasing bending moment. In the maximum moment region the increase in stress is less pronounced. The peak stress close to midspan is a stress concentration occurring at the pre-crack.

It is clear from the figure that when the width ratio increases the CFRP axial stress increases. The main reason for this is probably a 3D-effect in the beam width direction. For a small width ratio, see Fig.13a, there is a tendency that the CFRP carries the axial load in the centre part of the beam cross section and the steel carries the axial load in the left and right parts. For a large width ratio on the other hand, see Fig. 13b, there is CFRP directly beneath the steel, and hence the CFRP will take more part in carrying the load. The importance of this effect is related to the position of the steel bars; if the bars are more evenly distributed over the beam width the effect may be less pronounced.

Another reason may be that a larger width ratio implies a wider bond. Even though the CFRP stiffness is constant a larger width ratio implies a wider bond. This means a larger stiffness in the bond which leads to a faster increase in axial stress in the CFRP.

When a larger part of the axial stress is carried by the CFRP, steel yielding will take place at a higher external load level. Since steel yielding is often the initiation of the final fracture process this also means that the beam will be able to carry a larger load.

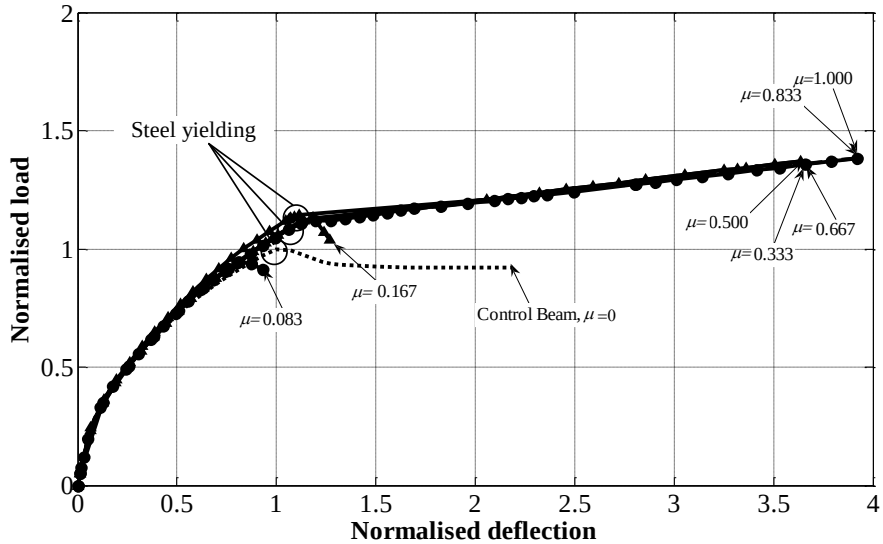

Fig. 9. Normalised load-deflection curves for different width ratios, μ, and constant stiffness, K=0.25K_o.

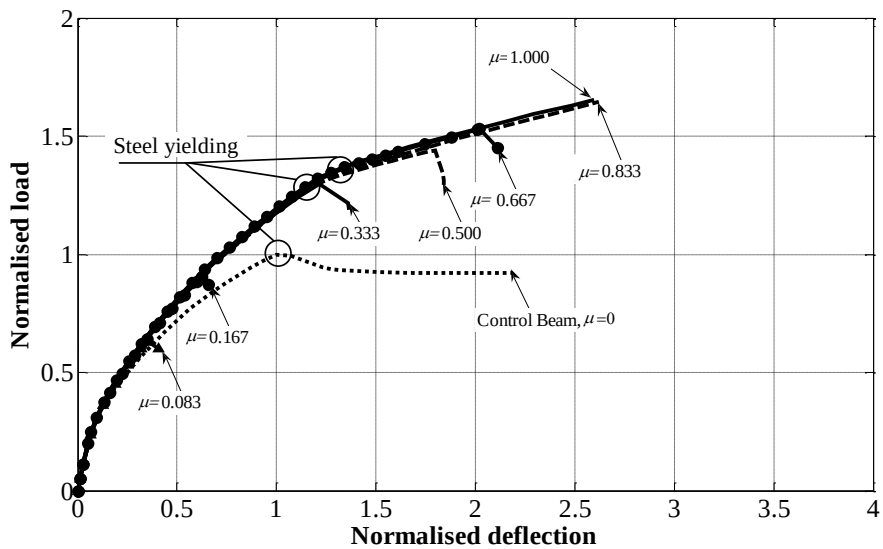

Fig. 10. Normalised load-deflection curves for different width ratios, μ, and constant stiffness, K=K_o.

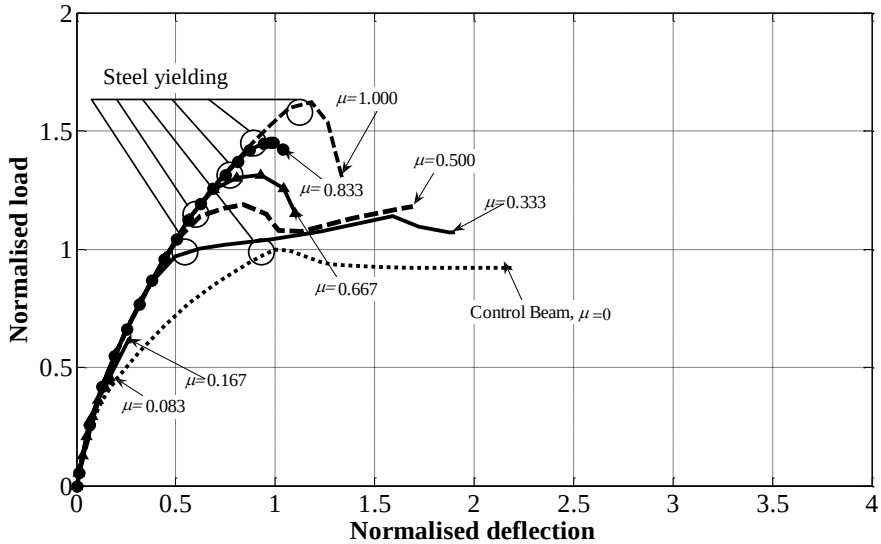

Fig. 11. Normalised load-deflection curves for different width ratios, μ, and constant stiffness, $K=4K_o$.

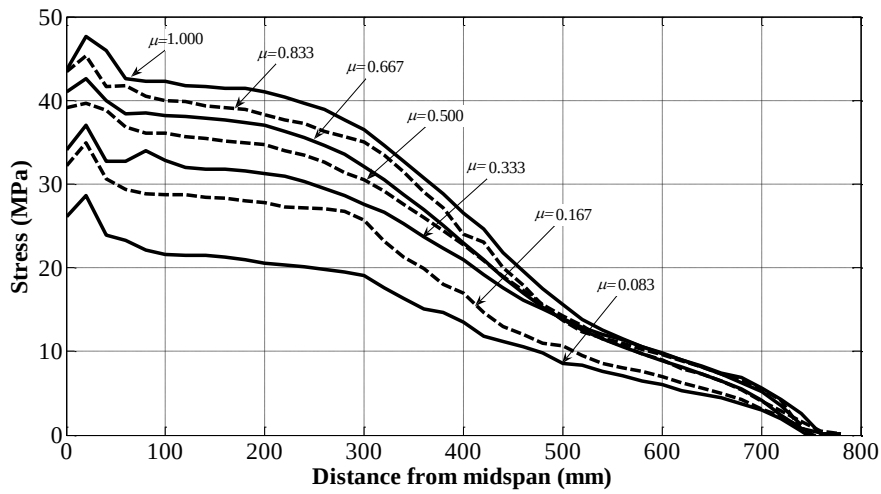

Fig. 12. Axial stress distribution in the CFRP plate at load 40 kN, for $4K_o$.

(a) Small width ratio (b) Large width ratio

Fig. 13. Comparison of geometry for small and large width ratios.

Fig. 14 illustrates the maximum load ratio for different values of stiffness and width ratio. It can be seen that for small width ratio with any value of stiffness, the maximum load ratio is less than 1, implying that a small width ratio will decrease, or at least not increase, the load bearing capacity of the beam. This is due to the debonding of CFRP before steel yielding, as mentioned before. For small stiffness with any value of the width ratio the load increases until a certain value of width ratio is reached, and then there is no further increase in load. This is due to the fact that the failure mode at this value of the width ratio shifts to rupture of CFRP, thus the use of large width ratio with small stiffness does not give any further increase of the maximum load. It is obvious that the medium stiffness with plate width equal to beam width gives maximum of maximum load ratio. The maximum value of α=1.78 was obtained for K=2K_o and μ=1. The cost of CFRP is probably not a critical factor, but it is still interesting that K=0.25K_o and μ=1 gives α=1.38. This means that 12.5% of the amount of reinforcement gives 78% of the maximum load ratio.

It can also be seen that for μ<0.5 the maximum load ratio increases with decreasing stiffness. This is due to the fact that debonding occurs earlier when increasing the stiffness with a small value of μ, then the utilization of CFRP decreases. For μ≥0.5 the maximum load ratio increases with stiffness of CFRP, until a certain value of the stiffness, and then it decreases due to the fact that debonding after this value occurs earlier.

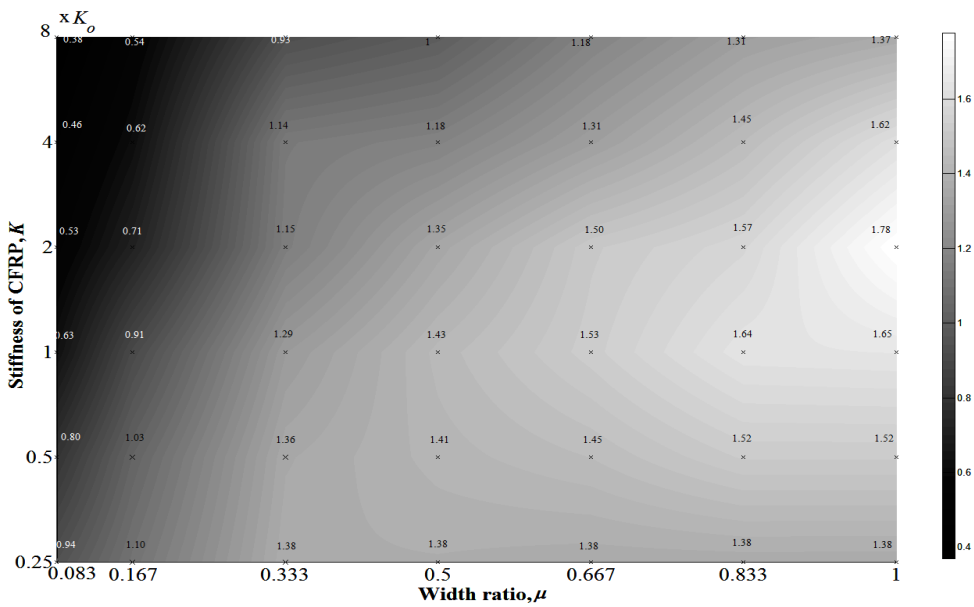

Fig. 14. Maximum load ratio, α, versus the width ratio, μ, and stiffness of CFRP, K. The scale indicates the maximum load ratio.

7.2. Group 2: Effect of varying CFRP width

In group 2 and 3 the starting point is the CFRP geometry used in the experimental study (w_{CFRP}=50 mm, t_{CFRP}=1.2 mm and E_{CFRP}=165 GPa). The results illustrate the effect of changing CFRP width (group2) and changing CFRP thickness (group3).

In group 2 the CFRP width is varied at constant thickness, implying that both the width ratio and stiffness vary, Fig. 6.

The beam stiffness increases with CFRP width. This is caused by the increase in CFRP stiffness, Figs. 9-11. Beams with small CFRP width fail at low load as was previously noted. The maximum load increases with CFRP width. This implies that the effect of increased width ratio (which generally increases the maximum load) is stronger than the effect of increased stiffness (which decreases the maximum load for the values of K and μ used here).

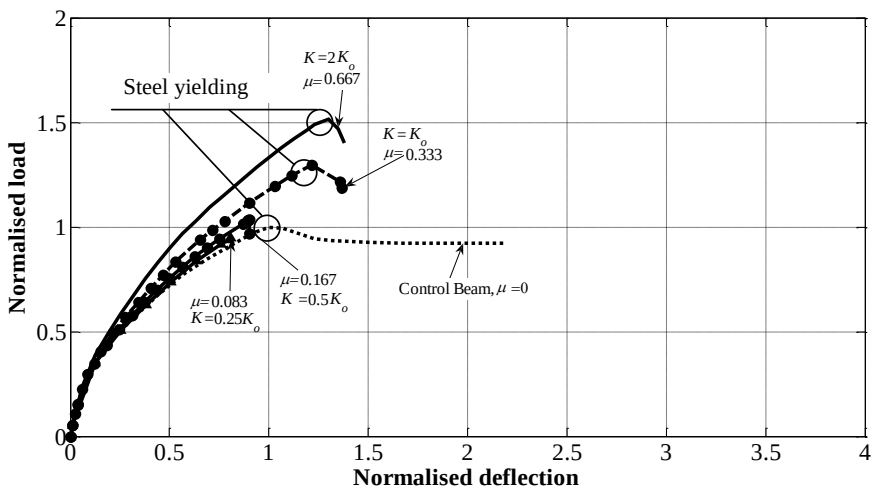

Fig. 15. Normalised load-deflection curves for different width ratios at constant thickness.

7.3. Group 3: Effect of varying CFRP thickness

In group 3 the CFRP thickness is varied at constant width, implying that CFRP stiffness is varied but the width ratio is kept constant.

As shown in Fig. 16, the maximum load ratio increases up to a certain value of the stiffness and then decreases. This is due to the same reasons as mentioned in section 7.1. A higher value of the maximum load ratio is however obtained here compared to Fig. 14, due to a higher resolution in the input values. It is interesting to note that when increasing the amount of external reinforcement by increasing the thickness, the maximum load ratio does not always increase as in the previous section. This means that it is preferable to increase the amount of reinforcement by increasing the width of CFRP rather than increasing the thickness. For example it is better to attach two CFRP plates side by side than on top of each

other. As mentioned before, for small thickness (stiffness) the failure mode was CFRP rupture while for large thickness it was debonding. This result supports what Toutanji, et al. [22] found.

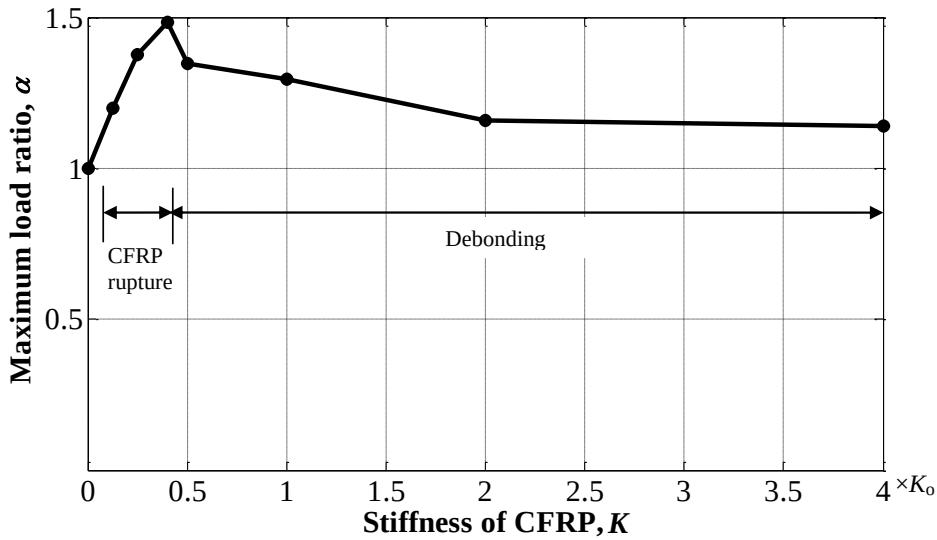

Fig. 16. Maximum load ratio versus stiffness of CFRP at constant width ratio.

8. Conclusion

A finite element model accounting for material non-linearity has been developed and successfully verified against experimental work. A parametric study has been performed to study the effects of stiffness and width of CFRP. The following conclusions are drawn:

- An increase in CFRP stiffness always gives an increase in beam stiffness.
- Different failure modes will occur depending on the values of CFRP stiffness and width ratio. High stiffness and low width ratio will result in debonding failure before steel yielding due to stress concentration at the plate end. This failure occurs at a small load value and should always be avoided.
- When the CFRP stiffness is small, there will be CFRP rupture after steel yielding. In this case, the width ratio will not have an influence on the maximum load. No clear conclusion can be made regarding if a higher maximum load will be obtained or not if the CFRP stiffness is increased to the extent that CFRP rupture will no longer occur. For some width ratios there is an increase in maximum load and for others there is a decrease.
- For medium stiffness and medium to high width ratio, debonding failure will occur after steel yielding. Debonding may initiate at the plate end or at a flexural crack and will in some cases include concrete splitting.

- Maximum load ratio increases with increasing CFRP stiffness until a certain value of the stiffness, thereafter the maximum load ratio decreases with increasing CFRP stiffness. The higher the width ratio, the higher is the optimal CFRP stiffness.
- Except when CFRP rupture is the limiting phenomenon, a higher width ratio will always give a higher maximum load ratio. One reason for this is that a high width ratio will decrease stress concentrations which otherwise may limit the load bearing capacity. Another reason is that a high width ratio will lead to that a larger part of the axial load is carried by the CFRP, which means that steel yielding will occur at a higher external load.
- The best maximum load ratio obtained in this study was 1.78, and it was reached for a CFRP stiffness of $2K_o$ and a width ratio of 1.

9. References

1. Ai-hui, Z., Wei-Liang, J., & Gui-bing, L. Behaviour of preloaded RC beams strengthened with CFRP laminates. Journal of Zhejiang University Science A 2006; 436-444.
2. Ashour, AF., El-Refaie, S.A., and Garrity, SW. Flexural strengthening of RC continuous beams using CFRP laminates. Cement & Concrete Composites 2004; 26: 765- 775.
3. Esfahani, M., Kianoush, M., & Tajari, A. Flexural behaviour of reinforced concrete beams strengthened by CFRP sheets. Engineering Structures 2007; 29: 2428-2444.
4. Pham, H., & Al- Mahaidi, R. Experimental investigation into flextural retrofitting of reinforced concrete bridge beams using FRP compoistes. Composite Structures 2004; 66: 617-625.
5. Camata, G., Spacone, E., & Zarnic, R. Experimental and nonlinear finite element studies of RC beams strengthened with FRP plates. Composites: Part B 2007; 38: 277-288.
6. Coronado, C. A., & Lopez, M. M. Sensitivity analysis of reinforced concrete beams strengthened with FRP laminates. Cement and Concrete Composites 2006; 28: 102-114.
7. Ebead, U., & Marzouk, H. Tension - stiffening model for FRP strengthend RC concrete two-way slab. Materials and Structures 2004; 193-200.
8. Lundquist, J., Nordin, H., Täljsten, B., & Olafsson, T. Numerical analyis of concrete beams sterengthened with CFRP- A Study of anchorage lengths. In: FRP in Construction, Proceeding of The International Symposium of Bond Behaviour of FRP in Structures. 2005; 247-254.
9. Pannirselvam, N., Raghunath, P., & Suguna, K. Strength Modeling of Reinforced Concrete Beam with Externally Bonded Fibre Reinforcement Polymer Reinforcement. American J. of Engineering and Applied Science 2008; 1(3): 192-199.
10. Obaidat,Y., Heyden, S., & Dahlblom, O. The Effect of CFRP and CFRP/Concrete Interface Models when Modelling Retrofitted RC Beams with FEM. Composite Structures, 2010; 92: 1391–1398.

11. Obaidat,Y. Retrofitting of reinforced concrete beams using composite laminates, Master Thesis, Jordan University of Science and Technology. 2007.
12. Hibbitt, Karlsson, Sorensen, & Inc. ABAQUS Theory manual, User manual, Example Manual, Version 6.7. Providence, RI, 2000.
13. ACI Comitte 318. Building Code Requirements for Structural Concrete and Commentary (ACI 318-99). American Concrete Institute, Detroit, MI, 1999..
14. Beton, C. E.-I. CEB-FIP Model Code 1990 (CEB-FIP MC90). Bulletin D'Information , No.215, Lausanne, 1993.
15. Hillerborg, A. The theoretical basis of a method to determine the fracture energy G_f of concrete. Materials and Structures, RILEM 50-FMC, 1985; 108, pp 291-296.
16. Saenz, L. Discussion equation for the stress - strain curve of concrete. By Desayi P, Krishnan S. ACI J 1964; 61:1229–35.
17. Hu H.-T., Schnobrich W.C. Constitutive modelling of concrete by using nonassociated plasticity. J Mater Civil Eng (ASCE) 1989;1(4):199–216.
18. Camanho, P. P., and C. G. Davila. Mixed-Mode Decohesion Finite Elements for the Simulation of Delamination in Composite Materials. NASA/TM-2002–211737, 2002; 1-37.
19. Lu, X. Z., Ten, J. G., Ye, L. P. and Jaing, J. J. Bond-slip models for FRP sheets/plates bonded to concrete. Engineering Structures 2005; 24 (5): 920-937.
20. JCI. Technical report on continous fibre reinforced concrete. JCI TC952 on Continous Reinforced Concrete 1998; 116-124.
21. JCI. Technical report on retrofit technology for concrete structures. Technical Committee on Retrofitting Technology for Concrete Structures 2003; 79-97.
22. Toutanji, H., Zhao, L., and Zhang, Y. Flexural behavior of reinforced concrete beams externally strengthened with CFRP sheets bonded with an inorganic matrix. Engineering Structures March 2006; 28: 557-566.